Applied Catalysis A, General 594 (2020) 117419

Contents lists available at ScienceDirect

Applied Catalysis A, General

journal homepage: www.elsevier.com/locate/apcata

Minimizing energy demand and environmental impact for sustainable NH_3 and H_2O_2 production—A perspective on contributions from thermal, electro-, and photo-catalysis

Justin S.J. Hargreaves[a,*], Young-Min Chung[b,*], Wha-Seung Ahn[c,*], Takashi Hisatomi[d], Kazunari Domen[d,e,*], Mayfair C. Kung[f,*], Harold H. Kung[f,*]

[a] School of Chemistry, University of Glasgow, Glasgow G12 8QQ, Scotland, United Kingdom
[b] Department of Nano & Chemical Engineering, Kunsan National University, 558 Daehak-ro, Kunsan, Jeollabuk-Do 54150, Republic of Korea
[c] Department of Chemistry and Chemical Engineering, Inha University, Incheon 402-751, Republic of Korea
[d] Research Initiative for Supra-Materials, Interdisciplinary Cluster for Cutting Edge Research, Shinshu University, 4-17-1 Wakasato, Nagano 380-8553, Japan
[e] Office of University Professor, The University of Tokyo, 7-3-1 Hongo, Bunkyo-ku, Tokyo 113-8656, Japan
[f] Department of Chemical and Biological Engineering, Northwestern University, Evanston, IL 60208, U.S.A.

ARTICLE INFO

Keywords:
Hydrogen peroxide synthesis
Ammonia synthesis
Electrocatalysis
Photocatalysis
Catalyst selectivity
Catalyst stability

ABSTRACT

There is an urgent need to provide adequate and sustainable supplies of water and food to satisfy the demand of an increasing population. Catalysis plays important roles in meeting these needs by facilitating the synthesis of hydrogen peroxide that is used in water decontamination and chemicals production, and ammonia that is used as fertilizer. However, these chemicals are currently produced with processes that are either very energy-intensive or environmentally unfriendly. This article offers the perspectives of the challenges and opportunities in the production of these chemicals, focusing on the roles of catalysis in more sustainable, alternative production methods that minimize energy consumption and environmental impact. While not intended to be a comprehensive review, the article provides a critical review of selected literature relevant to its objectives, discusses areas needed for further research, and potential new directions inspired by new developments in related fields. For each chemical, production by thermal, electro-, and photo-excited processes are discussed. Problems that are common to these approaches and their differences are identified and possible solutions suggested.

1. Introduction

Adequate supplies of water, energy, and food to satisfy an expanding population are essential to sustainable global development and maintaining world peace. These needs are intertwined in a complex manner. For example, the food sector accounts for about 30 % of total global energy consumption and 20 % of greenhouse gas (GHG) emissions [1], even though almost 800 million people still suffer from hunger [2]. In addition, agriculture is responsible for 69 % of global freshwater withdrawal [3]. Without question, there is an urgent need to implement environmentally benign processes that could reduce the demands for energy and natural resources in meeting the dual needs for food and water. Catalysis will play important roles in these processes.

This perspective article is intended as a springboard for discussion of the future roles of catalysis in the syntheses of two high volume commodity chemicals: ammonia and hydrogen peroxide. In addition to the fact that these two chemicals are critical in sustaining the global supply of food and water via fertilizer production and wastewater clean-up, respectively, they are also playing increasingly prominent roles in the move towards greener synthesis of chemicals. H_2O_2 is a preferred oxidant in many chemical syntheses as it produces water as the benign byproduct. An example is the commercial process to produce propylene oxide (the HPPO process) using H_2O_2 with a titanium silicalite catalyst [4]. As another example, ammonia together with hydrogen peroxide are being actively explored for ammoximation to produce oximes using Ti silicalite catalysts [5]. There are recent reports of using these two chemicals to react with small ketones to form low-carbon-chain nitroalkanes [6].

The current processes to produce these two chemicals, unfortunately, have significant environmental impact. Ammonia is manufactured by the energy intensive Haber-Bosch process using catalysts that facilitate the reaction of nitrogen with hydrogen. Although direct

* Corresponding authors.
E-mail addresses: Justin.Hargreaves@glasgow.ac.uk (J.S.J. Hargreaves), ymchung@kunsan.ac.kr (Y.-M. Chung), whasahn@inha.ac.kr (W.-S. Ahn), domen@shinshu.u-tokyo.ac.jp (K. Domen), m-kung@northwestern.edu (M.C. Kung), hkung@northwestern.edu (H.H. Kung).

https://doi.org/10.1016/j.apcata.2020.117419
Received 22 October 2019; Received in revised form 13 January 2020; Accepted 16 January 2020
Available online 26 January 2020

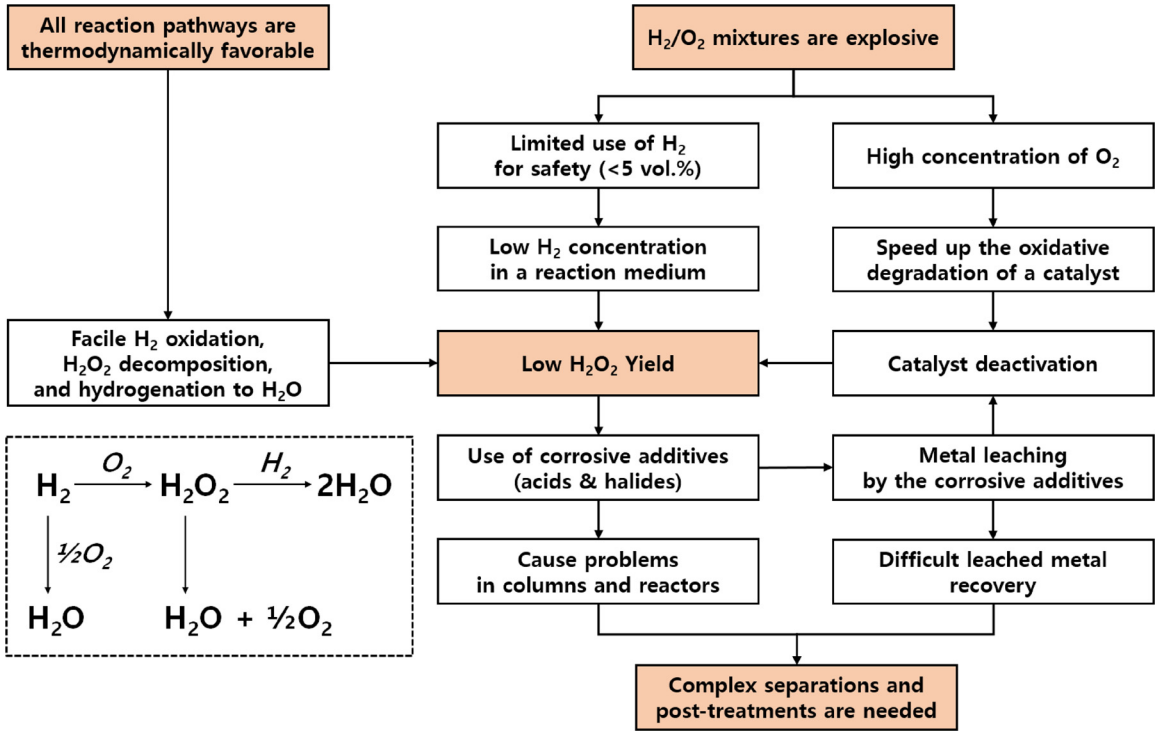

Fig. 1. Challenges in the direct synthesis of H_2O_2 from H_2 and O_2.

combination of N_2 with H_2 to form NH_3 is thermodynamically favorable at standard state (ΔG°_f = -16.2 kJ mol^{-1} at 25 °C), the slow kinetics necessitates operation at elevated temperatures of 350–500 °C where the thermodynamics becomes less favorable (ΔG°_f = 27.1 kJ mol^{-1} at 427 °C), and high pressures ranging from 20 to 40 MPa. The H_2 source is derived from reforming of hydrocarbons using processes that also entail high temperatures. For example, the principal route for hydrogen production in the U.S. is steam reforming of methane, which is thermodynamically favorable only above ~530 °C, when the reaction is highly endothermic (ΔH°_{rxn} = 222 kJ mol^{-1}). The U.S. Department of Energy estimates recently that the on-site energy consumption for ammonia production in the country amounts to ~200 × 10^{15} J a^{-1} (J/year) based on a production of 15 × 10^6 t (metric tonnes) in 2018 (14 × 10^3 kJ/kg) [7]. For a global annual production of 170 × 10^6 t [8], the global annual process energy consumption would be 10^{18}-10^{19} J, which is 1–2 % of the total global energy consumption of 5.9 × 10^{20} J.

H_2O_2 is a versatile and powerful oxidant used as an environmentally friendly oxidant for chemical synthesis as well as in the advanced oxidation process (AOP) for decontamination of water by mineralizing dissolved organics through oxidation. The global production of H_2O_2 is 4.5 × 10^6 t in 2014 [9], and about 10 % of it is produced in the U.S. (3.9 × 10^5 t in 2010 [10]). More than 95 % of H_2O_2 is synthesized by the anthraquinone process that involves auto-oxidation of hydrogenated anthraquinone or its derivatives [11]. The process poses significant environmental burden due to the need to regenerate hydrogenated anthraquinone and separation and purification of the produced H_2O_2 from large quantities of organic solvents and catalysts. It is also energy-intensive, consuming 16 × 10^6 J/kg even though the overall process ($H_2 + O_2 = H_2O_2$) is thermodynamically favorable and requires no energy input ($\Delta G^\circ_f = -2.6 \times 10^6$ J kg^{-1}, $\Delta H^\circ_f = -5.5 \times 10^6$ J kg^{-1}) [10].

Thus, reducing the energy demand and decreasing the ecological footprint in the production of these two chemicals would contribute to sustainable global development. In this perspective article, both thermal and photo/electrochemical processes in ammonia and hydrogen peroxide production are discussed. Although thermal processes are well developed, there is room for further improvement with the advent of recent new understanding in catalyst structure-property relationships. The historic economic disadvantages of electrocatalytic synthesis due to high cost of electricity relative to petrochemical fuels and feedstocks are no longer valid as the cost of renewable electricity has lowered consequent of advances in materials, engineering, and efficiencies in capturing solar and wind energy [12,13].

This article is not intended to be a comprehensive review of catalysis on the production of these two chemicals, since there are many excellent recent reviews on the direct synthesis of hydrogen peroxide [11,14–17] and ammonia synthesis [16,18–28]. Instead, the article focuses on potential roles and research opportunities to improve existing catalysts and production methods that have not been commercialized. Thus, review of the literature will be critical but brief and confined to those directly relevant to the ensuing discussion. For H_2O_2, production by direct synthesis with H_2 and O_2 (i.e. reduction of O_2 with H_2), reduction of O_2 with simultaneous oxidation of another molecule which may form a useful co-product, and photoelectrochemical (PEC) oxidation of H_2O will be discussed. For NH_3 production, the discussion centers on improving the catalyst in the Haber-Bosch process and exploring the alternative nitride looping process, and the potential for photo/electrochemical production.

2. H_2O_2 production

2.1. Thermal catalysis

2.1.1. Direct H_2O_2 production from H_2 and O_2

The direct synthesis of hydrogen peroxide (DSHP) from H_2 and O_2 offers the simplest route and the highest atom utilization efficiency of all known processes. It has been explored as an alternative to the commercial anthraquinone process. One particularly interesting aspect is the direct, *in situ* production in which the H_2O_2 formed is used immediately without separation or purification, and thus offering potentially significant cost reduction. For example, *in situ* production of H_2O_2 could reduce the raw material cost for propylene oxidation to propylene oxide by up to 45 %, and the total production cost by 24 % compared with using purified H_2O_2 [29]. However, there are significant barriers

that need to be overcome before the benefits of DSHP can be realized. These barriers include the danger of explosion with a H_2/O_2 mixture and the competition by various facile side reactions, such as decomposition of H_2O_2, hydrogenation of H_2O_2, and oxidation of H_2 to H_2O that adversely affect the H_2O_2 yield (Fig. 1). If H_2O_2 is produced in the presence of organic compounds, H_2O_2 oxidation of the organics also needs to be minimized. To overcome these issues, there is intensive ongoing research that focuses on the design of efficient catalysts and processes to accommodate the requirements for commercial applications [11,15,30–32].

It is widely accepted that the key reaction steps of the DSHP include (i) dissociation of adsorbed H_2 molecule to H atoms on an active metal surface, (ii) formation of a *OOH intermediate by reaction of the H atom with an adsorbed O_2 molecule (where * denotes an active site), and (iii) formation and desorption of H_2O_2 by reaction of *OOH intermediate with another H atom. In order to attain high H_2O_2 selectivity, it is essential to suppress the dissociation of the O—O bond, which results in reactive intermediates such as *O or *OH that eventually leads to wasteful H_2O formation. It is equally important to prevent the subsequent, thermodynamically feasible side reactions of decomposition and hydrogenation of produced H_2O_2. For example, it has been reported that for Pd/C, H_2O_2 hydrogenation is as much as 3–4 times faster than H_2O_2 decomposition, decreasing the H_2O_2 selectivity by 70–85 % [33]. Therefore, an ideal catalyst should selectively promote H_2O_2 formation without also promoting these unwanted side-reactions. The approaches being investigated include fine-tuning the physicochemical properties of the active metals via bimetal formation, addition of modifiers, and/or modifying the particle size, phase, and electronic structure. For practical purposes, improving the stability of the catalyst and understanding the effect of the reaction medium are equally important.

There has been impressive improvement in recent years in the catalyst performance for DSHP. However, there is insufficient detailed understanding of the underlying reasons for the improvement because experiments performed to identify the best catalysts generally utilize metal particles of a distribution of sizes with different exposed crystal planes and, for bimetallic catalysts, particles with a range of compositions. Model catalysts that are structurally and compositionally defined have been employed to generate in-depth understanding. Since Pd is considered the most active metal for DSHP, it is the most heavily studied.

2.1.1.1. Nature of the active sites. It has been shown that H_2O_2 production activity depends on the exposed crystal planes of Pd. The premise is that crystal planes where O—O bond scission is suppressed favors high selectivity for H_2O_2. Zhou and Lee synthesized colloidal Pd particles in the presence of ionic polymers to obtain particles with different preferentially exposed crystal planes, and demonstrated that the (110) planes exhibited higher H_2O_2 selectivity compared with the (100) and (111) planes [34]. Kim, et al. compared SiO_2-supported Pd nanocubes with exposed (100) planes and nanooctahedra with (111) exposed planes, and found the nanooctahedra to be more selective for H_2O_2 production than the nanocubes at similar conversions [35]. They noted that the observation of a higher selectivity for the (111) than the (100) surface planes agrees with the DFT computational results of O_2 adsorption and dissociation on low index planes of Pd, which showed that the barrier for O_2 dissociation was higher on a Pd (111) surface than on (110) or (100) [36]. Unlike adsorption on the (100) or (110) planes, adsorption of O_2 on Pd (111) leads mostly to placing two surface O atoms that are closer to each other than the molecular dissociation distance, thus encouraging associative adsorption which favors production of H_2O_2 [36].

It should be noted that although it is established that the atomic structure of the exposed plane of an active metal critically influences catalytic performance, the detailed arrangement of metal atoms of a desired active site for H_2O_2 formation remains unresolved. Shape control of an active metal particle can be challenging in practice. The most stable surface under reaction conditions may be different from the one most selective for H_2O_2 formation. The effect of support, especially on the geometric and electronic properties of the active metal needs to be examined and understood.

The dependence of selectivity on the structure of the exposed plane likely contributes to the observed particle size dependence. It was reported that on a series of Pd/hydroxyapatite, samples with $1-2$ nm particles were much more selective than those with larger particles, whereas samples with isolated Pd were inactive [37]. The higher selectivity of the $1-2$ nm particles was attributed to the presence of higher ratios of $Pd^{\delta+}/Pd^{o}$ with the support stabilizing the partially charged Pd atoms. However, Burch et al. [38] observed that for supported Pd catalysts, generally the reduced catalysts exhibited higher H_2 conversion activity and H_2O_2 selectivity. Flaherty et al. [15] noted an absence of an induction period for H_2O_2 formation with Pd nanoparticles whereas a noticeable induction period existed for PdO particles, suggesting a need to reduce the PdO for activity. These apparent variant in observations suggests the potential that there exists an optimal ratio of ionic and metallic Pd and their distribution/location on the surface. The challenge is to identify this optimum, devise a system to maintain it under reaction conditions, and understand the underlying reaction mechanism. Such an understanding should also improve our ability to identify beneficial modifiers to Pd, such as halides and a second metal.

2.1.1.2. Effect of catalyst modifiers. A mechanism for H_2O_2 production involves formation of η^2-adsorbed O_2 and its subsequent hydrogenation to *OOH [39]. Thus, catalyst modifiers that alter the stability and/or barrier to the formation of these species would affect the reaction. DFT computational results suggest that the energy barrier for hydrogenation of *OOH is lower than for O—O bond scission on isolated Pd atoms but not on ensembles [40]. Thus, modifiers that break up Pd ensembles should be beneficial. In addition, modifiers that can reduce the extent of electron back-donation to $2\pi^*$ orbitals of adsorbed O_2 would also reduce the tendency for O—O bond cleavage [15]. This mechanistic interpretation may explain in part the effect of chloride and bromide modifiers. In an acidic solution, these halides greatly suppress H_2O_2 decomposition or hydrogenation while exhibiting much milder effects on H_2O_2 formation [41]. It should be noted that other halides, such as iodide or fluoride are much less effective. That is, additional study is needed to fully understand the effect of halide modifiers.

Ligands and bimetallics are used also to modify the Pd active sites. Ligands or surfactants are often used in colloidal preparation to control the shape of metal particles. In one example, hexadecyl-2-hydroxyethyldimethyl ammonium dihydrogen phosphate ($C_{20}H_{46}NO_5P$) was used as a stabilizing and reducing agent to prepare Pd colloidal particles deposited onto a carbon support. Compared to naked Pd particles on carbon, the stabilized Pd catalyst showed a higher H_2O_2 selectivity [42]. It was suggested that on the surface modified with surfactant molecules, the peroxyl intermediate adsorbed in a vertical configuration instead of lying flat on the Pd surface, making cleavage of the O—O bond more difficult. The activation barrier for the hydrogenation of the *OOH intermediate to H_2O_2 was lower than the barrier for over-hydrogenation to water, and the desorption of the product was energetically advantageous over its further hydrogenation and/or decomposition.

A number of modifying metals have been reported to be beneficial for Pd, including Au, Pt, Ag, Sn, Zn, and others [43–45]. The pioneering work of Hutchings and coworkers highlighted the potential for bimetallic catalysts [43], and AuPd seems to be one of the most efficient active metal combinations. In this system, Au acts as an electronic modifier of Pd. It decreases the rates of H_2O formation much more than H_2O_2 formation, resulting in an increase in H_2O_2 selectivity [46]. In the case of a Pd/C catalyst, modifiers that block H_2O_2 decomposition sites on the carbon support surface also contribute to selectivity

enhancement [47]. These sites could originate from impurities. Density functional theory (DFT) calculations suggest that Au may inhibit the activation of H_2 and dissociation of O_2, *OOH, and H_2O_2, and the AuPd may be an optimum bimetallic in terms of activity and selectivity [17,44]. Because the binding energies of O, OH, and OOH on a metal surface scale proportionally to each other [48–50], an optimal catalyst for H_2O_2 formation activity would need to have an intermediate binding strength of H and O. Other metal modifiers such as Ni, Zn, or Sn that are beneficial probably exert similar geometric and electronic effects on the active sites of Pd [51–53].

Recently, Freakley et al. reported that in the Pd system, small metallic particles (< 4 nm) could be encapsulated more readily than larger particles with a thin (< 2 nm) layer of an amorphous oxide, such as Sn oxide, that are inactive for H_2O_2 decomposition or hydrogenation. The encapsulation greatly suppressed the H_2O_2 degradation activity of these particles [54]. Larger particles, though not encapsulated, could be made to produce H_2O_2 with high activity and selectivity by partial oxidation of the surface Pd. Thus, by designing an oxidation-reduction-oxidation cycle to achieve both encapsulation of small particles and partial oxidation of larger ones, they obtained active and selective catalysts. This positive effect by encapsulation with oxide clusters was also observed with Ni, Ga, Zn, Co, and In modifiers. Interestingly, unlike the PdSn system, the oxidation-reduction-oxidation cycle was not beneficial for the AuPd/TiO_2 system [54], possibly because Au oxide is unstable at high temperatures and would not form an inactive Au oxide layer similar to Sn.

The above examples point to the importance of understanding the transformation of catalysts upon pretreatment and during reaction. Instead of comparing catalysts at a fixed reaction time, collecting temporal information would facilitate identification of the nature of the active sites, an important piece of information for catalyst development that is not commonly collected. For example, information from *in situ* characterization or, at least, after reaction would help explain the changes observed on a AuPd/TiO_2 catalyst that the initial rate of H_2O_2 production was 114 mol h^{-1} kg^{-1} catalyst and the initial H_2O_2 selectivity was 93 %, but deteriorated to 66 and 60 %, respectively, after 30 min [55].

In addition to modifiers and bimetallics, the reaction medium also plays an important role. The presence of gaseous H_2 suppresses significantly the rates of decomposition of H_2O_2 to H_2O and O_2 on both Au-Pd [56] and Pd catalysts [41]. The presence of protons is also very important. Protic acids are essential for the beneficial effect of Cl^- and Br^- [41]. Under identical conditions, H_2O_2 formation rate is much lower in an aprotic than a protic solvent [46]. This suggests the possibility that hydrogenation of either *OO or *OOH may involve simultaneous proton and electron transfer from the catalyst to the adsorbate [39].

2.1.1.3. Catalyst stability. During operation, metal leaching is a concern. The primary cause of leaching is the strong ligation of surface metal atoms by species in the reaction medium. Metal ions and atoms at highly coordination unsaturation sites such as corners are particularly vulnerable. Metal leaching can be serious in strong acids and the presence of halide ions [41]. It was reported that stacking polyelectrolyte multilayers (PEMs) on a sulfonated resin can mitigate active metal leaching and enhance the H_2O_2 yield [57,58]. Continuous production up to 100 h of 8–10 wt% H_2O_2 was achieved by using Pd nanoparticle catalysts either encapsulated in or immobilized on the PEMs (Fig. 2).

2.1.2. Electrocatalytic synthesis

Direct synthesis of H_2O_2 from H_2 and O_2 can also be achieved electrochemically at room temperature or below by combining two half-cell reactions:

$H_2 \rightarrow 2H^+ + 2e^-$ at anode

$2H^+ + 2e^- + O_2 \rightarrow H_2O_2$ at cathode

Because the overall reaction is thermodynamically favorable, the system can operate as a fuel cell to generate electricity during H_2O_2 production (Fig. 3) [59]. In early work, H_2O_2 was generated under short-circuit conditions, using Au mesh and graphite membrane cathodes [60]. However, the resulting H_2O_2 concentration was limited to 59 mM (0.2 wt%) and the current efficiency (that is, the selectivity for H_2O_2 based on the quantity of H_2 reacted) was 10 % over a span of 10 h. This relatively poor performance was due to the low activity of the cathodes and low concentrations of O_2 in the catholyte. Subsequent work improved the catalyst and the delivery of O_2 [61]. For example, a cathodic catalyst prepared by pyrolysis of 0.05 wt.% Co-porphyrins (e.g. Co-TPP; TPP: 5,10,15,20-tetrakis(phenyl)-21H,23H-porphyrin) on vapor-grown carbon-fiber (VGCF) substrates achieved a production of pH-neutral, pure, 4.0 M (13.5 wt%) aqueous H_2O_2 solutions [62]. Another report using an optimized carbon-based support gave a H_2O_2 concentration of 5.5 M (18.7 wt%) in conjunction with a current efficiency of 55 % and estimated H_2O_2 concentrations greater than 30 wt% by increasing the current efficiency from 55 % to 90 % [63]. Similar to thermal catalytic DSHP, competition by over-reduction of O_2 to H_2O and decomposition of H_2O_2 remain challenges to high yields and efficient utilization of H_2.

It is also possible to produce H_2O_2 electrochemically by coupling the two-electron reduction of O_2 ($O_2 + 2\,H^+ + 2\,e^- \rightarrow H_2O_2$) with four-electron oxidation of H_2O ($2\,H_2O \rightarrow O_2 + 4\,H^+ + 4\,e^-$), using electrical energy to overcome the unfavorable thermodynamics of the overall reaction $2\,H_2O + O_2 \rightarrow 2\,H_2O_2$ ($\Delta G^0 = 116.7$ kJ mol^{-1}). For this set of reactions, the minimum potential required is 0.60 V. Although this voltage is lower than that for H_2O splitting ($H_2O \rightarrow H_2 + 0.5\,O_2$, 1.23 V), efficiency loss owing to decomposition of H_2O_2 remains a challenge. Alternatively, H_2O_2 can also be produced by coupling the two-electron reduction of H_2O ($2\,H^+ + 2\,e^- \rightarrow H_2$) and two-electron oxidation of H_2O ($2\,H_2O \rightarrow H_2O_2 + 2\,H^+ + 2\,e^-$) to give the net reaction $2\,H_2O \rightarrow H_2 + H_2O_2$. The minimum voltage required at the standard condition is 1.77 V at room temperature. This is greater than that for water electrolysis (1.23 V). Thus, there is efficiency loss by the competing reaction of H_2O electrolysis in addition to decomposition of H_2O_2.

2.1.3. Formation during parallel catalytic oxidation

The formation of H_2O_2 in the liquid phase in parallel with oxidation of organics has been reported some time ago. Instead of reducing the O_2 with H_2 as in DSHP, an organic reductant is used with concomitant formation of an oxidized organic product. Although in principle this can be accomplished in the gas phase, available literature has been confined only to the liquid phase. Because energy-demanding separation would be needed to produce pure solutions of H_2O_2, the parallel-production process is best applied in the form of *in situ* generation of H_2O_2 that is used immediately for selective oxidation to produce high-value products as the end goal, e.g. for selective epoxidation.

An obsolete industrial process to produce H_2O_2 in parallel with oxidation of an organic compound involved autooxidation of 2-propanol [64,65]. Currently, the predominant industrial process for H_2O_2 production is the anthraquinone autooxidation process that involves the cycle of hydrogenation of anthraquinone to anthrahydroquinone and its oxidation back to anthraquinone, while producing H_2O_2 [66]. On the other hand, catalytic selective oxidation of hydrocarbons or other reductant other than H_2 with parallel formation of H_2O_2 is much less studied. Only a limited number of catalytic systems have been reported in the literature, which include palladium (II) acetate-catalyzed oxidation of terminal alkenes to ketones in an organic solvent [67,68], 2-octanol oxidation [69], aqueous phase oxidation of glycerol catalyzed by Au/C [70], and oxidation of CO catalyzed by Au/TiO_2 [71] and Au/Calgon [72].

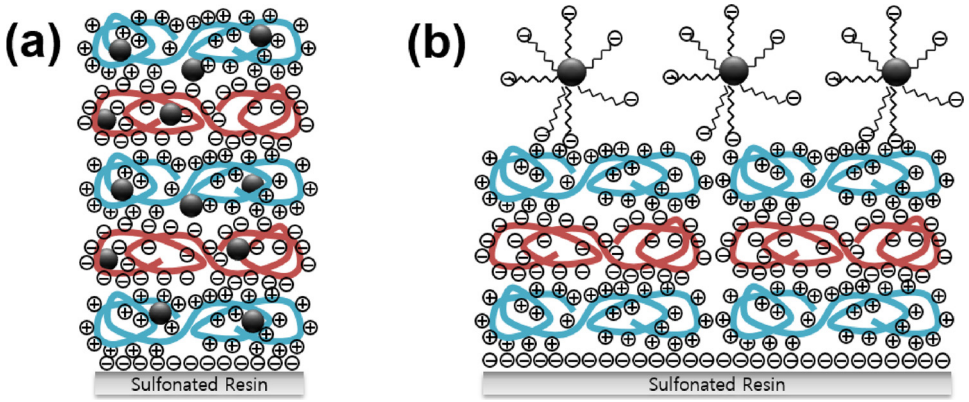

Fig. 2. Pd nanoparticles (a) encapsulated in and (b) immobilized on the polyelectrolyte multi-layers (PEMs) constructed on a sulfonated resin [57,58].

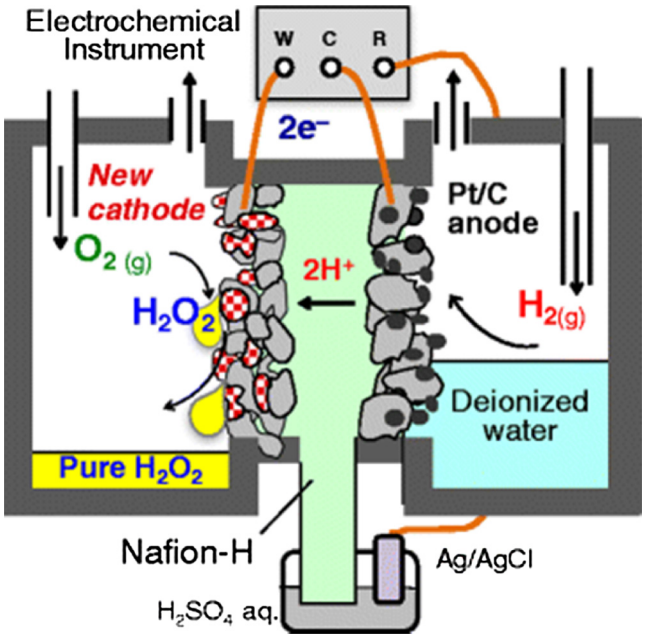

Fig. 3. Schematic diagram of fuel cell reactor intended for synthesis of pure aqueous H_2O_2 solutions. Reprinted from Ref. [63]. © 2017, Springer Science Business Media, LLC.

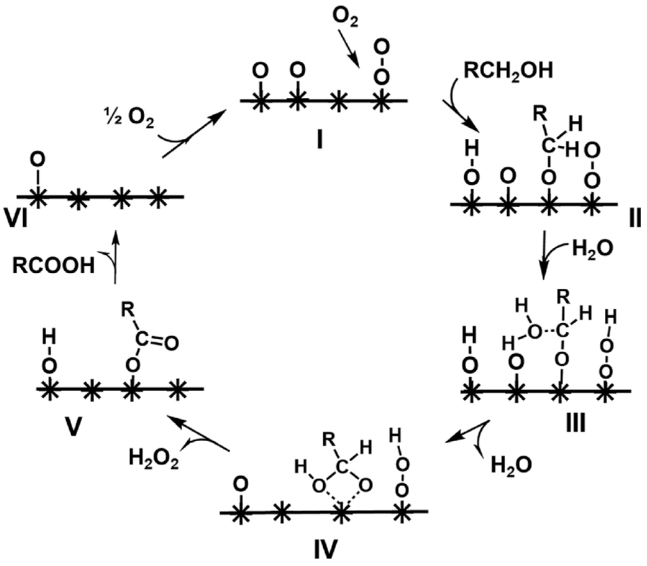

Fig. 4. A feasible mechanism for the heterogeneous catalytic H_2O_2 formation with co-oxidation of an organic alcohol. An O_2 molecule is adsorbed to form a peroxyl (I), which is hydrogenated to a hydroperoxyl (III) by the α C—H of the alcohol. Nucleophilic attack by H_2O in concert with cleavage of the second C—H bond results in an adsorbed carboxylate (IV) and desorption of H_2O_2. This mechanism accounts for results of isotopic labelling experiments, that the O atoms of H_2O_2 originate from O_2, and the O atoms of the acid originate from H_2O and alcohol.

The proposed mechanism for the Pd-complex catalyzed reaction involves first activation of O_2 to form a peroxy ligand on the metal. Insertion of the peroxy into a metal-hydride bond forms a hydroperoxy ligand [73,74], which is hydrogenated or hydrolyzed to form H_2O_2 [75]. Similar to DSHP, retaining the O—O bond in the O_2 molecule is believed to be essential. There is little mechanistic information for heterogeneous catalytic processes, but a mechanism that includes retention of the O—O bond and the formation of adsorbed peroxy intermediate, leading to the subsequent formation of peroxide is consistent with isotopic labelling results of the Au-catalyzed CO oxidation-assisted selective oxidation of propylene to propylene oxide. It was observed that ^{18}O-labelled propylene oxide was formed exclusively when $^{18}O_2$ was used but none when $H_2{}^{18}O$ was used [71]. Since it is reasonable to assume that propylene oxide is formed by reaction of propylene with H_2O_2 that is formed *in situ*, the labelling experiments suggest that H_2O_2 is formed directly from O_2. Various mechanisms that retain these essential features have been postulated [76]. Interestingly, when H_2O_2 was formed during oxidation of glycerol, ^{18}O was found in the glyceric acid product only when $H_2{}^{18}O$ was used but not with $^{18}O_2$ [70]. That is, the H_2O_2 formed was not consumed by glycerol oxidation. Instead, conversion of glycerol to glyceric acid involves nucleophilic attack at the C—O by H_2O or *–OH derived from H_2O. The information can be used as a starting point to postulate a mechanism, such as that shown in Fig. 4.

2.1.4. Opportunities and challenges for thermal and electrocatalytic processes

Among the processes discussed in this section, the DSHP process is the most studied and much more information is available for this catalytic system than the others. Thus, our discussion will center on the DSHP process while commenting on extension to other processes and focus on possible directions to explore and the knowledge gap for improving catalyst activity, selectivity, and stability. The important catalytic steps for discussion include activation of O_2, selective hydrogenation of O_2, and degradation of H_2O_2.

For processes that rely on reduction of O_2, which include DSHP, formation in parallel with oxidation of organics or CO, and electrochemical reduction of O_2, it is important to activate the O_2 molecule without dissociating the O—O bond. Thus, they would benefit from modifiers and surface atomic structures that reduce the M—O bond

strength and weakens the tendency of electron donation from the catalyst to the π* orbital of the adsorbed O_2 molecule. These processes may differ in the hydrogenation step of the adsorbed O_2. In DSHP, H_2 is dissociatively adsorbed on a catalyst and both H atoms are utilized in H_2O_2 formation by insertion into the surface M−O bond without dissociating the O−O bond. For production by parallel oxidation, the H atoms are derived from the organic molecules directly. Thus, the ability of a catalyst to cleave a C−H bond and facilitate hydride transfer to the $*O_2$ without cleaving the O−O bond is essential. If the H atom is derived from a proton and the ancillary electron, a situation that applies to electrochemical processes, the electronegativity of the surface that determines the potential for electron transfer to the adsorbed O_2 and proton is important, and the potential is expected to depend on the chemical nature of the surface and the morphology at the atomic scale [77,78]. Understanding this dependence is needed to predict the effects of catalyst/electrocatalyst modifiers. In all cases, the need to be able to transfer a H atom to O_2 without cleaving the molecule remains an essential criterion. It is important to better understand how these properties depend on the surface morphology, metal particle size, and the metal oxidation state distribution. More detailed characterization under catalytically relevant conditions would be highly desirable, especially *in situ* characterization.

There has been significant effort to optimize the addition of acid and halide promoters [31,38,39,79,80]. Chloride and bromide ions are generally used to suppress the degradative decomposition and hydrogenation of H_2O_2. Protons are necessary for the observed effects of halide ions on H_2O_2 formation activity [15,31]. Unfortunately, rules for the effects of these promoters are not yet available, and at times combination of catalysts, additives, and reaction conditions may lead to adverse effects. Apparently, the reaction mechanism becomes more complex and therefore difficult to predict upon addition of multiple promoters.

The support material plays an important role in these reactions and offers an avenue to catalyst improvement. Ideal support materials for H_2O_2 production should either be sufficiently inert to retain the intrinsic characteristics of the active metal or, preferably, offer synergistic effects with the active metal, as well as be inactive for any of the undesirable side reactions. Therefore, judicious selection of a suitable supporting material is as important as fine-tuning the active metal properties. In this regard, it is not understood why a carbon-supported Pd, Au, or Au-Pd catalyst is less active than their counterparts on titania, magnesia and alumina supports [81]. In the literature, a large number of support materials have been explored that possess: (i) well-ordered textural properties to minimize the mass transfer resistance of reactants, (ii) selective adsorption sites for anionic/cationic metal precursors to increase the metal dispersion and stability, and/or (iii) acidic functional groups or immobilized halide ions to eliminate the use of inorganic acids or halides [31,81,82].

Carbon material is perhaps the most popular and widely studied support for a variety of catalyst designs for DSHP, due to its low cost, ready availability, inertness, and stability in the presence of caustic additives. Carbon-supported catalysts are also employed for the parallel oxidation process, and due to its high electrical conductivity, for the electrochemical processes. To overcome the shortcomings of conventional activated carbons, such as the heterogeneous nature of the surface and irregular microporous structures, ordered mesoporous carbons have been tested, and their superior textural properties led to improved catalytic activities by reducing the diffusion resistance of the reactants [83].

Other efforts to improve catalytic performance of catalysts associated with carbon materials include modifying their properties by incorporating nitrogen or oxygen groups. N-incorporated carbon supports provide selective adsorption sites for the anionic Pd precursors, which led to the formation of small, monodispersed metal nanoparticles. Heterocyclic N species around the supported Pd nanoparticles withdraw electron density and modify the electronic properties of Pd species. By virtue of these two beneficial effects, the Pd catalyst supported on N-containing carbon nanotubes showed promising activity in DSHP [84]. However, it is important to minimize formation of amine/imine groups during the N-incorporation on the carbon supports because the basic sites may accelerate H_2O_2 decomposition [41,85]. Likewise, care needs to be exercised when modifying the surface of carbon materials by acid treatments. Although the acid-treated carbons may act as a solid acid support and be efficient in suppressing H_2O_2 decomposition [47], excessive acid treatment could have adverse effects such as destruction of the pore structure, enhanced hydrophilicity of the surface, and active site poisoning by carboxyl groups [86,87]. It should be cautioned that the relationship between H_2O_2 decomposition activity and pH has not been firmly established.

Solid acid supports have been extensively investigated as means to prevent equipment corrosion and metal leaching caused by aqueous acids. These include inorganic oxides, carbon materials, organic/inorganic molecular sieves, heteropoly acids, metal-organic frameworks (MOFs), and resins [87–91]. For industrial applications, sulfonated resins offer several advantages: large-scale production with competitive price and easy control of the acid concentration. Active site blocking or diffusion limitation to molecular fluxes caused by the irregular pore structure of the highly crosslinked resin structure can be reduced by swelling the matrix in a polar solvent. As illustrated in Fig. 5, however, the matrix may become de-crosslinked slowly by the produced H_2O_2. Decomposition of the resin releasing polysulfonic acid (PSA) may also occur. The latter decreases the catalytic activity, and the PSA is difficult to remove via conventional solid-liquid separation techniques. In propylene epoxidation, PSA may significantly decrease the PO selectivity by catalyzing the ring opening of epoxide when *in situ* generated H_2O_2 is used.

MOFs are an emerging, important class of solid acid support materials, because they can be prepared to possess high concentrations of robust Lewis acid sites at the metal nodes and Brønsted acid sites at the organic linkers introduced by post-synthesis modifications [92]. Indeed, Pd catalysts supported on acidic and highly stable MOFs such as MIL-101-SO_3H and UiO-66-SO_3H showed superior catalytic activity to Pd/HBEA (SiO_2/Al_2O_3 = 25) [91]. However, prolonged contact of the MOF with generated H_2O_2 during reaction leads to partial and gradual oxidative decomposition of the MOF structure. Partial deformation of the MOF structure by H_2O_2 was also reported [93].

It is unlikely that modifying the acidity/basicity of or addition of halide to the support could be applied to the parallel oxidation process involving organic alcohols unless the highly basic reaction condition can be eliminated. Likewise, MOFs might not be useful unless structures immune to destruction in a strongly basic medium or new chemistry can be found that can proceed at near neutral conditions.

Innovative support designs should be pursued to prevent the subsequent degradation reaction of the generated H_2O_2. For DSHP, one approach is to encapsulate a metal particle with a thin, size-selective carbon coating that permits hydrogen diffusion through to the metal but not oxygen. In this manner, the metal dissociates the H_2 molecule and the H atoms formed spillover onto the carbon layer, where hydrogenation of O_2 to H_2O_2 occurs. By preventing O_2 from accessing the metal, the degradative pathway initiated with dissociation of O_2 on the metal and the accompanying side reactions are avoided. Preliminary investigations demonstrated that a thin carbon coating on Pt nanoparticles allows preferential diffusion of H_2 to the Pt surface over O_2, thereby greatly reducing O−O dissociation (Fig. 6). Consequently, the O_2 molecules react with the spilt-over hydrogen that diffuses from the Pt to the carbon coating to form H_2O_2. Moreover, the carbon layer is also efficient in suppressing the access of generated H_2O_2 to the Pt surface. Therefore, this thin carbon coating increases the H_2O_2 selectivity at the expense of rate of H_2 conversion due to the increased mass transfer resistance [94].

In addition to activity and selectivity, the stability of a catalyst is also of critical importance. In the liquid phase, metal leaching resulting

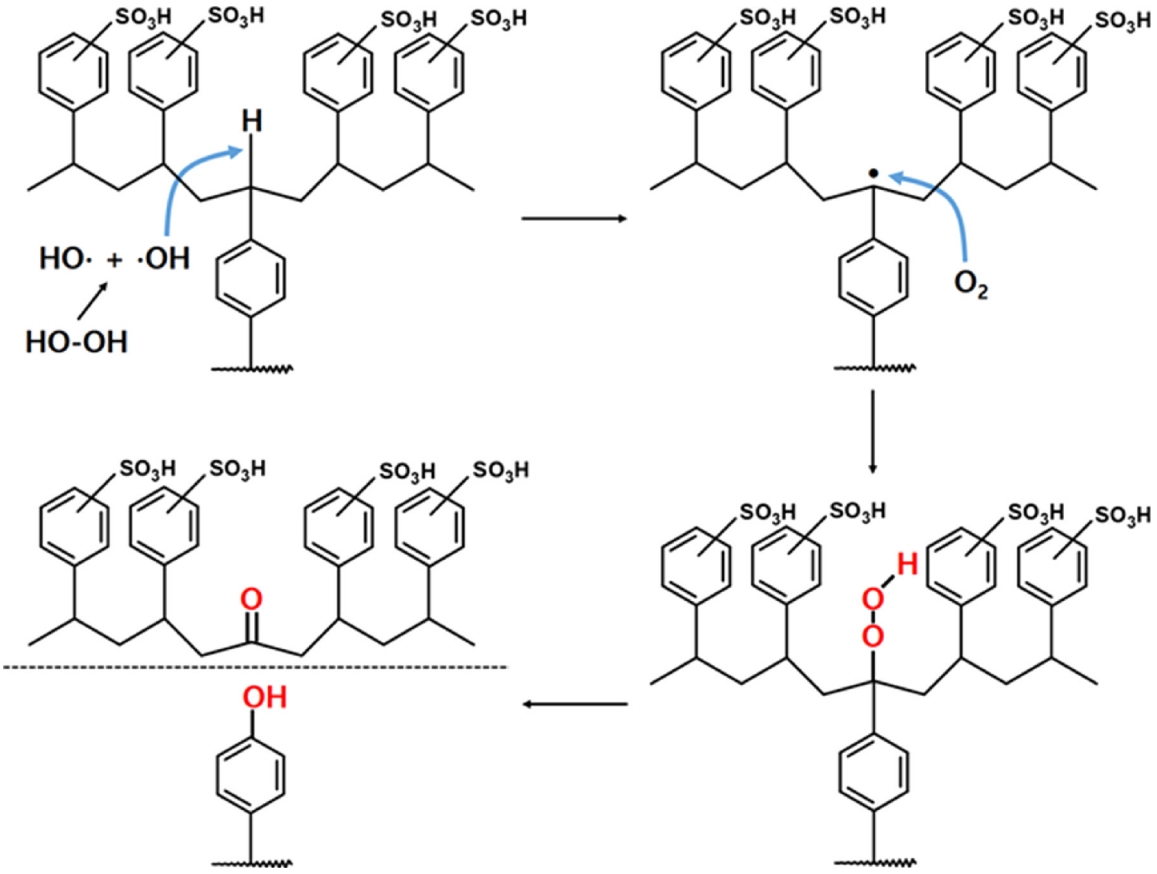

Fig. 5. De-crosslinking mechanism of a sulfonated resin by H_2O_2 and O_2.

in performance degradation is a common issue. Coating also offers the potential benefit of enhancing catalyst stability by reducing metal leaching for processes in an aqueous medium as well as metal sintering. This is particularly useful when the DSHP process is used in tandem processes for chemical production in the presence of base metal catalysts. In general, leaching of base metals such as iron, cobalt, copper, and manganese is more severe than noble metals. For example, leaching of Cu [95], Fe [96], and Co [97–99] during catalytic oxidation has been reported, and the resulting liquid containing the leached metal ions may become toxic. On the other hand, no leaching of Au was detected in the oxidation of phenol [100], although there was leaching during oxidation of neat cyclooctene [101]. It has been reported that an overcoat of Al_2O_3 deposited on Cu/Al_2O_3 prevented Cu leaching because the overcoat interacted strongly with the under-coordinated copper atoms that are more susceptible to leaching [102]. Similarly, a yolk-shell structure of Co@C-N prevented Co leaching because of the stabilizing interaction between the Co nanoparticles and the C-N nanosheets [103].

Metal sintering is another source of deactivation of catalysts that can be mediated by coating. For example, encapsulating Au nanoparticles with a carbonaceous shell hinders crystallite growth [104] and there are many literature examples of other combinations of components. Another strategy for catalyst stability utilizes strong interactions between catalyst components to anchor the active phase (such as metal

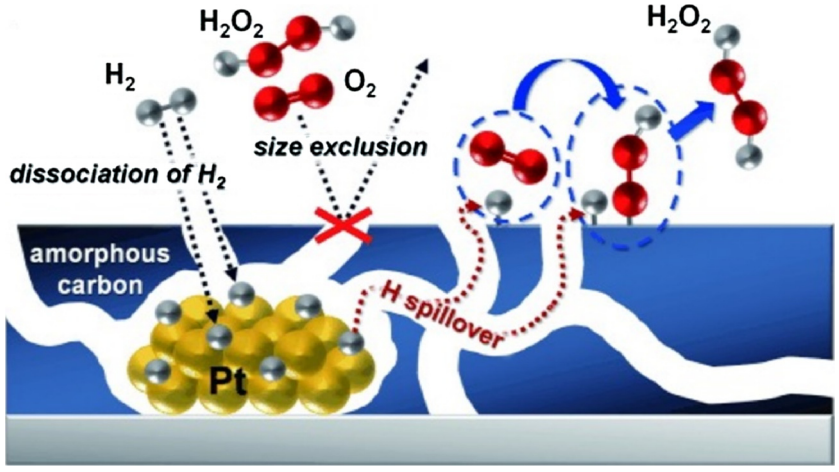

Fig. 6. Pt catalysts covered by amorphous carbon layers that allow the selective diffusion of H_2 over O_2. Reprinted from [94] with permission from Wiley-VCH.

particles). For example, the particle growth of Ru on supported catalysts in aqueous solutions was found to be related to the bulk electronegativity of the support, with sintering rate decreasing in the order of $SiO_2 > C \approx TiO_2 > \gamma\ Al_2O_3$ [105]. This is attributed to the Ru-O-M (M = support cation) interaction that is influenced by the electron density on the oxygen which in turn is affected by the electronegativity of the support cation. Another observation is that cobalt leaching was less severe with $CoFe_2O_4$ than cobalt oxide due to the strong Fe-Co interactions in $CoFe_2O_4$ [106].

For oxide-supported catalysts, hydrolysis and redeposition of the support oxide could result in phase transformation and/or loss of surface area and cause sintering and/or encapsulation of the supported metal particles. This has been documented with common supports such as γ-Al_2O_3 [107]. Understanding the chemistry of leaching and degradation and devising preventive methods are research opportunities. Our current understanding is that the susceptibility of a support oxide to dissolution may be related to the density of defects. Thus, stability can be enhanced by reducing the defect density. This has been observed with zeolites where capping the silanol defects with organosilanes improved the ability of the zeolite to maintain crystallinity in hot liquid water [108]. Coating of an oxide surface with a layer of more stable material is also effective. This has been observed with samples comprising an alumina coating on amorphous silica-alumina [109] and carbon coating of SBA-15 [110].

The effect of the reaction medium is not well understood. Whereas acidic solutions are beneficial for effective action of halide modifiers in DSHP, known examples of production in parallel with oxidation require highly basic solutions where the high hydroxide concentrations should make the system insensitive to halide modification. At present, the mechanistic implication of these differences has yet to be explored.

The nature of diluent gas for the H_2/O_2 mixture also exerts great influence on the catalytic activity for DSHP. CO_2 seems preferable to N_2 as measured by higher H_2O_2 selectivity and productivity, because it may act as a mild-acid promoter and increase the surface coverage of active sites with oxygen by increasing the amount of dissolved oxygen under high pressure [83,111]. However, the possibility of equipment corrosion by the carbonic acid, which is produced from CO_2 in the presence of water-containing solvent, is of concern for industrial applications.

For the DSHP reaction to be a real breakthrough for selective oxidation processes, the catalyst performance without using halide additives needs to be significantly improved. To develop an improved catalyst, a better understanding of the fundamental reaction kinetics and mechanism of the DSHP is needed. In this context, a standard test reaction protocol with a benchmarking catalyst will be desirable for meaningful comparison of the performance of different catalysts. In addition, advanced computational methods and *in situ* characterization techniques would help improve our understanding of the reaction mechanisms that depend on the catalyst and reaction conditions. In that regard, there have been noticeable advances in recent years [44,112]. However, the simple molecular structures and similar rotational/vibrational behaviors of the involved molecules limit the possibilities in *in situ* characterization, in particular the vibrational spectroscopic approaches.

The economic feasibility of the hydrogen peroxide-propylene oxide (HPPO) process depends on the cost of production and the market price of H_2O_2. Therefore, successful implementation of an integrated direct synthesis DS-HPPO process requires not only the continuous production of approximately 8–12 wt% H_2O_2 without additional purification steps, but also direct supply of the *in situ* generated H_2O_2 without any separation. Although successful development of the DS-HPPO process may open a new avenue for related industries, *i.e.,* PO, polyols, and polyurethane by substantially lowering the raw material cost, the performance of reported state of the art catalysts is still too poor for the DS-HPPO process in the absence of caustic additives. Therefore, at present, the use of caustic additives seems inevitable to meet the industrial target for H_2O_2 concentration, which obviously increases the fixed and operating costs of the process.

For H_2O_2 production in the parallel oxidation scheme, there are practical challenges: (1) For commercial viability, if H_2O_2 is to be sold as a purified product, the oxidation product of the parallel process needs to have appropriate economic value after separation. An alternative is to use the H_2O_2 *in situ* to produce a high-value product. (2) Ideally, every molecule in the parallel reaction is involved in H_2O_2 generation. (3) None of the H_2O_2 produced is degraded by decomposition to O_2 or hydrogenation to water. (4) The catalyst needs to be stable in the reaction solution mixture. The very limited information available thus far suggests that it is possible to achieve the limit of forming one H_2O_2 molecule for every molecule of alcohol oxidized in the parallel reaction absence of the subsequent decomposition of the formed H_2O_2. It would be even more attractive if every oxidation equivalent in the parallel reaction can be utilized for H_2O_2 production. Another serious problem with the very few systems studied is the significant degradation of the formed H_2O_2, thus limiting the overall productivity. Thus, there is much to be understood and improved for this process.

Other than CO, alcohols are the other reductant studied for H_2O_2 production in the parallel reaction. Anecdotal information suggests that aldehydes but not acids are also very effective. It is known that different C—H bonds have different ability to reduce O_2 to peroxy and peroxide, but a more comprehensive understanding would allow prediction of how effective a molecule could be to produce H_2O_2. Ideally, the parallel oxidation reaction would make use of low-cost renewable reactant and produce a high-value product. For example, coupling the dehydrogenation of propane to propene with the production of H_2O_2 ($\Delta G_{300K} = 119\ kJ\ mol^{-1}$) is thermodynamically feasible. In this case, propane functions as a hydrogen source to reduce O_2 to H_2O_2. An even more desirable hydrogen source is H_2O. However, the reaction $O_2 + 2H_2O = 2H_2O_2$ is thermodynamically uphill ($116.7\ kJ\ mol^{-1}$). Thus, it needs to be coupled with another reaction to overcome the thermodynamics. Table 1 lists some possibilities, unfortunately, the highly desirable oxidation of alkene to epoxide ($\Delta G^0_{rxn} \approx -115\ kJ\ mol^{-1}$) is not among them.

Similar to DSHP, suppressing the undesired H_2O_2 decomposition reaction is also very important during co-oxidation. At present it is not known whether formation and decomposition of H_2O_2 share the same active sites, and if there are methods to suppress decomposition without affecting formation. This could be addressed with more detailed understanding of the reaction mechanism.

2.2. Photoelectrochemical (PEC) synthesis

Photocatalytic and PEC approaches have the potential to eliminate the need to supply H_2 as a fuel or electrical energy because electrons and holes excited by the energy of light are available. They convert light energy to chemical energy. Similar to electrochemical methods, they both have two half-cell reactions, and the difference among them rests on the source of energy to achieve electron-hole charge separation: electrical potential for the electrochemical approach, and photon energy for the photocatalytic and PEC approaches. Photocatalytic production of H_2O_2 has been demonstrated for a long time. For example, excitation of ZnO or TiO_2 with UV radiation produces H_2O_2 in an

Table 1
ΔG^0_{rxn} of oxidation reactions (R + 0.5 O_2 = RO).

Reaction	ΔG^0_{rxn}, kJ/mol
Alkane to alcohol	≈ -140
Primary alcohol to aldehyde	≈ -200
Aldehyde to acid	-250 to -260
CO to CO_2	-222

aqueous medium, albeit with a rather low efficiency [113]. In order for this approach to be commercially attractive, higher efficiencies and use of visible light excitation are highly desirable.

2.2.1. Photocatalytic processes

One area of current interest is to discover/develop photocatalytic systems that utilize visible light. One such system is based on C_3N_4. Shiraishi et al. reported the production of H_2O_2 via photocatalytic reduction of O_2 on graphitic carbon nitride (C_3N_4) and related materials [114]. Earlier work showed that the conduction band potential of C_3N_4 was sufficiently negative to reduce O_2 to H_2O_2, but the valence band edge was not sufficiently positive to oxidize H_2O to O_2 efficiently. Thus, isopropanol was needed to serve as a sacrificial electron donor. Under these conditions, the Faradaic efficiency of the H_2O_2 production process reached 90 %, based on the mass balance of the oxidation products of isopropanol (acetic acid and CO_2). Modifying the C_3N_4 network by doping with the electron-deficient aromatic compound pyromellitic diimide (PDI) shifts the valence band edge to a more positive value [115], and the resulting PDI-doped C_3N_4 (C_3N_4/PDI) generated H_2O_2 from O_2-saturated water under visible light irradiation with an apparent quantum yield of 2.6 % at 420 nm. Further modification with reduced graphene oxide (RGO) [116] and boron nitride (BN) [117] as electron and hole collectors, respectively, improved the charge separation efficiency (Fig. 7), and the photocatalyst produced H_2O_2 at a solar-to-chemical conversion efficiency of 0.27 %. In this system, O_2 reduction and water oxidation were presumed to proceed on the RGO and BN, respectively, however, O_2 evolution by water splitting could not be confirmed because O_2 was also bubbled through the reaction solution.

Charge separation in C_3N_4 can also be enhanced by doping with biphenyl diimide (BDI) instead of PDI but with a significant difference [118]. Based on the calculated energy positions of the highest occupied and the lowest unoccupied molecular orbitals using DFT, both photoelectrons and holes in the C_3N_4/PDI system are generated in the same melem unit. In contrast, photoexcited holes are localized in the BDI unit while electrons remain in the melem unit in the C_3N_4/BDI system. For this reason, it is not necessary to modify C_3N_4/BDI with RGO and BN to promote charge separation. It has also been reported that mellitic triimide (MTI), having a three-directional planar structure, can be used in place of PDI (which has a two-directional planar structure) to produce dense sheets [119]. Compared to the PDI system, the C_3N_4/MTI system contains a higher density of melem units in its sheet structure and exhibits improved conductivity owing to the enhanced intra- and interlayer transport of photogenerated charge carriers. These C_3N_4-related photocatalysts have generated H_2O_2 to concentrations > 4 mM (140 ppm) [116]. The production of H_2O_2 from pure water using a $BiVO_4$ photocatalyst loaded with Au nanoparticles serving as active sites for the two-electron O_2 reduction reaction has also been demonstrated [120].

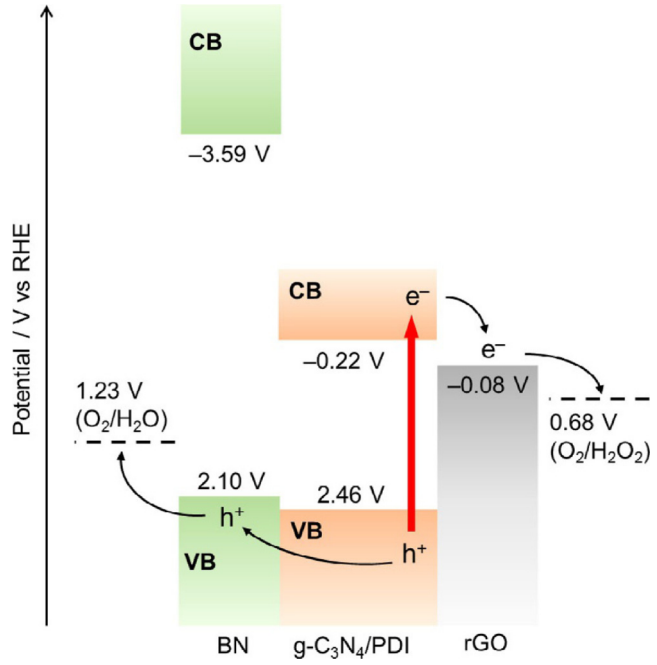

Fig. 7. Electronic band structures for g-C_3N_4/PDI, RGO and BN. Reprinted with permission from Ref. [117]. © WILEY-VCH Verlag GmbH & Co. KGaA, Weinheim.

2.2.2. Photoelectrochemical processes

An emerging PEC system is based on $BiVO_4$. In their pioneering work [121], Fuku and Sayama examined PEC water oxidation using $BiVO_4$/WO_3 bilayer photoanodes prepared on glass substrates coated with fluorine-doped tin oxide (FTO) in solutions of various electrolytes, including sulfate, phosphate, borate and bicarbonate. These $BiVO_4$/WO_3/FTO photoanodes (hereafter referred to simply as $BiVO_4$ photoanodes) were found to generate exceptionally high photocurrents in an aqueous bicarbonate solution. In addition, H_2O_2 was produced at an appreciable concentration in an anolyte when the catholyte and anolyte were separated by a proton exchange membrane and bicarbonate was employed as a supporting electrolyte. Bicarbonate ions were reported to be electrochemically oxidized to percarbonate ions, after which these ions would undergo spontaneous hydrolysis to regenerate bicarbonate, giving H_2O_2 as the overall product [122,123]. A similar reaction mechanism would be feasible on $BiVO_4$ photoanodes in response to photoexcitation, where bicarbonate ions are adsorbed and oxidized to percarbonate, followed by hydrolysis to produce H_2O_2 and regeneration of bicarbonate in the electrolyte solution. Accordingly, bicarbonate ions can be regarded as a catalyst for the two-electron oxidation of water to H_2O_2. Interestingly, $BiVO_4$ itself has also been shown to function as an electrocatalyst for H_2O_2 production by water oxidation in the absence of light irradiation [123], while Bi_2O_3, V_2O_5 and many other binary oxides (except for Al_2O_3 and TiO_2) lower the H_2O_2 production rate. Thus, it appears that the unique electrochemical characteristics of the $BiVO_4$ surface may have specific functions in promoting the PEC production of H_2O_2. It was suggested by DFT calculation that the surface of $BiVO_4$ had a moderate formation energy for adsorbed OH (*OH) species and was favorable for H_2O_2 production [50]. Too strong or too weak binding of *OH would result in the sequential oxidation of H_2O_2 into O_2 via the four-electron oxidation or the formation of OH radical ($OH^{\cdot}$) species via the one-electron oxidation, respectively By increasing the bicarbonate electrolyte concentration and bubbling CO_2 through the electrolyte solution (to lower the pH), the Faradaic efficiency of H_2O_2 production on $BiVO_4$ photoanodes reached a maximum of 54 % and a H_2O_2 concentration of 2 mM (68 ppm).

The Faradaic efficiency of H_2O_2 production on $BiVO_4$ photoanodes can also be improved by surface modification of the anode with oxide coatings, such as SiO_2, ZrO_2, TiO_2 and Al_2O_3, formed by spin coating of metal-organic solutions and subsequent calcination (Fig. 8) [124]. Among these oxides, Al_2O_3 is the most effective, and has been shown to increase the Faradaic efficiency from 54 % to 80 %. The deposited Al_2O_3 forms a mesoporous layer on the surface of the $BiVO_4$ photoanode and suppresses the sequential PEC oxidation of H_2O_2 to O_2 on the anode. It has been suggested that H_2O_2 generated on the $BiVO_4$ surface diffuses into the electrolyte solution through this mesoporous Al_2O_3 layer, likely by concentration gradient. The weak acidity of the Al_2O_3 surface may also enhance adsorption of the weakly basic bicarbonate ions. Thus, $BiVO_4$ photoanodes modified with Al_2O_3 are able to evolve H_2O_2 from dilute aqueous solutions of bicarbonate. It was found further that using chemical vapor deposition (CVD) to apply a thinner conformal Al_2O_3 coating than by dip-coating impeded the photocurrent less while maintaining the beneficial effects of the Al_2O_3 [125].

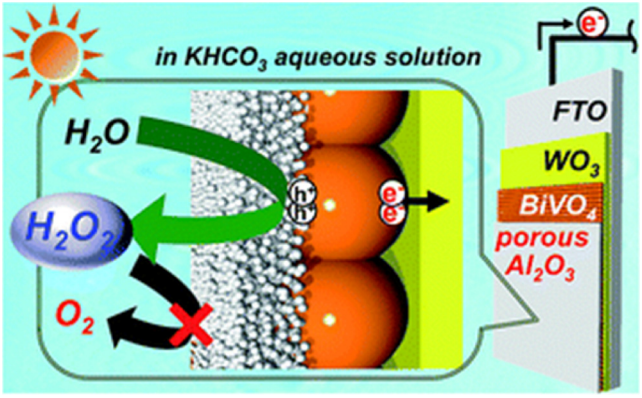

Fig. 8. Schematic showing the PEC generation of H_2O_2 from H_2O on an Al_2O_3/$BiVO_4$/WO_3/FTO photoanode under solar light irradiation. Reprinted with permission from Ref. [124]. Copyright 2017, The Royal Society of Chemistry.

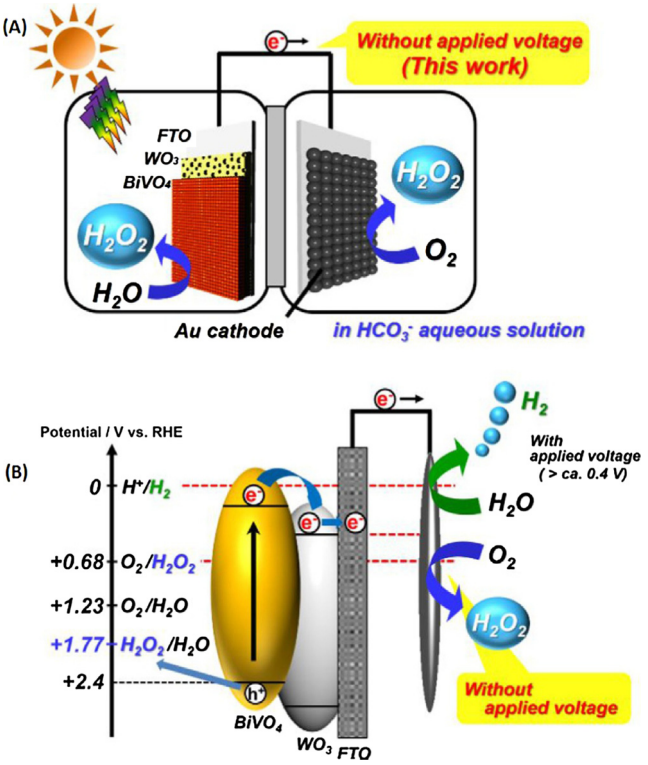

Fig. 9. (A) Diagram of a photoelectrode system for producing only H_2O_2 via the two-electron oxidation of H_2O on a WO_3/$BiVO_4$ photoanode under solar light irradiation. (B) The energy diagram for the photoelectrode system. Reprinted with permission from Ref. [126]. © 2017, WILEY-VCH Verlag GmbH & Co. KGaA, Weinheim.

The potential of the conduction band edge for $BiVO_4$ is lower than the reversible hydrogen evolution potential (0 V vs. RHE). Therefore, it is necessary to apply an external voltage or combine a $BiVO_4$ photoanode with photovoltaic cells or photocathodes to drive the PEC H_2O_2 and H_2 evolution reactions. Alternatively, O_2 can be reduced to H_2O_2 by two-electron reduction on the cathode [126]. The reversible potential for this reaction is +0.68 V vs. RHE, which is more positive than the conduction band edge potential for $BiVO_4$. Thus, photoexcitation of a $BiVO_4$ photoanode in conjunction with a H_2O_2-evolving cathode can spontaneously produce H_2O_2 by water oxidation with the simultaneous reduction of O_2 (Fig. 9), achieving the overall reaction: $O_2 + 2\ H_2O \rightarrow 2\ H_2O_2$. The reported faradaic efficiencies for H_2O_2 production on a $BiVO_4$ photoanode was 50 % and on a cathode 90 % based on an FTO-coated electrode modified with Au nanoparticles under short-circuit conditions.

2.2.3. Challenges and opportunities

The production of H_2 is perhaps the most useful process for solar-to-chemical energy conversion as H_2 can be used as a fuel and chemical feedstock. Solar splitting of water also produces O_2, which has a rather low market value (about \$0.1 kg^{-1}, less than one-tenth that of H_2) [127]. In contrast, the price of H_2O_2 is much higher (\$0.7–1.2 kg^{-1} in 2009) [9]. Therefore, co-production of H_2 and H_2O_2 by water oxidation instead of O_2 is much more attractive economically [128]. The oxidation of water into H_2O_2 also has other benefits. For example, H_2O_2 is produced in the liquid phase and spontaneously separated from the co-produced gaseous H_2. The reversible potential for the two-electron oxidation of water to H_2O_2 is +1.77 V vs. RHE, higher than the +1.23 V for the four-electron oxidation to O_2. If PEC water splitting into H_2 and H_2O_2 proceeds with the same quantum efficiency and the product H_2O_2 can be collected efficiently, this reaction would yield a solar-to-chemical energy conversion efficiency 1.4 times greater than water splitting into H_2 and O_2. Materials with wider band gaps (*i.e.*, shorter absorption edge wavelengths) are necessary to split H_2O into H_2 and H_2O_2, although this will not be a major problem because most common oxide semiconductors have valence band edges at potentials more positive than the reversible potential for the two-electron oxidation of water [129].

To date, the semiconductors applied to H_2O_2 production under visible light have been limited to C_3N_4-related materials and $BiVO_4$, which have relatively large bandgap and can utilize only the higher energy portion of the solar spectrum. Thus, it would be helpful to explore the applicability of smaller band-gap semiconductor materials to determine the surface properties essential for efficient H_2O_2 evolution, and to allow the development of more efficient PEC and photocatalytic systems. For both PEC and photocatalytic systems, it is especially vital to improve the physical electronic properties of the semiconductors so as to efficiently utilize photoexcited carriers [130].

Particle transfer technology can be used to facilitate the survey of various well-crystallized particulate semiconductors in PEC reactions [131]. As an example, photoelectrodes comprising particulate semiconductors fabricated by particle transfer have been applied to the direct PEC production of methylcyclohexane, a promising H_2 carrier, from toluene (Fig. 10) [132]. Suppression of the sequential decomposition of H_2O_2 on the catalyst and support remains an important challenge because H_2O_2 is an intermediate product regardless of whether it is generated reductively or oxidatively. Thus, catalysts and surface modification layers should be developed for the current PEC and photocatalytic systems to promote H_2O_2 production and suppress sequential decomposition. Sayama et al. developed an Al_2O_3 coating that blocked the access of H_2O_2 in the electrolyte solution to the $BiVO_4$ photoanode [124,125], and a similar effect has been obtained by applying an amorphous transition metal oxide coating to overall water splitting photocatalysts [133]. Such coatings allow O_2 evolved on the photocatalyst surface to diffuse into the reaction solution while blocking the access of H_2O_2 in the reaction solution to the photocatalyst. The modification of photocatalysts and photoelectrodes with such coating layers may improve selectivity for H_2O_2 production,

It is equally essential that these semiconducting materials are stable in the aqueous and acidic or basic environment under light irradiation. Oxidation of the photoelectrode material facilitated by light is another challenge. Coating layers could also serve as a protection layer. Some oxynitride photocatalysts evolve not only O_2 but N_2 as an oxidation product during the overall water splitting reaction because of the self-oxidation of nitride ions (N^{3-}). Fortunately, modification with amorphous oxide layer can suppress it and enable oxynitride photocatalysts to split water into H_2 and O_2 at the stoichiometric ratio [134]. Note that H_2O_2 is an efficient hole scavenger and is readily oxidized to water [135]. It is therefore essential to use surface modification layers with

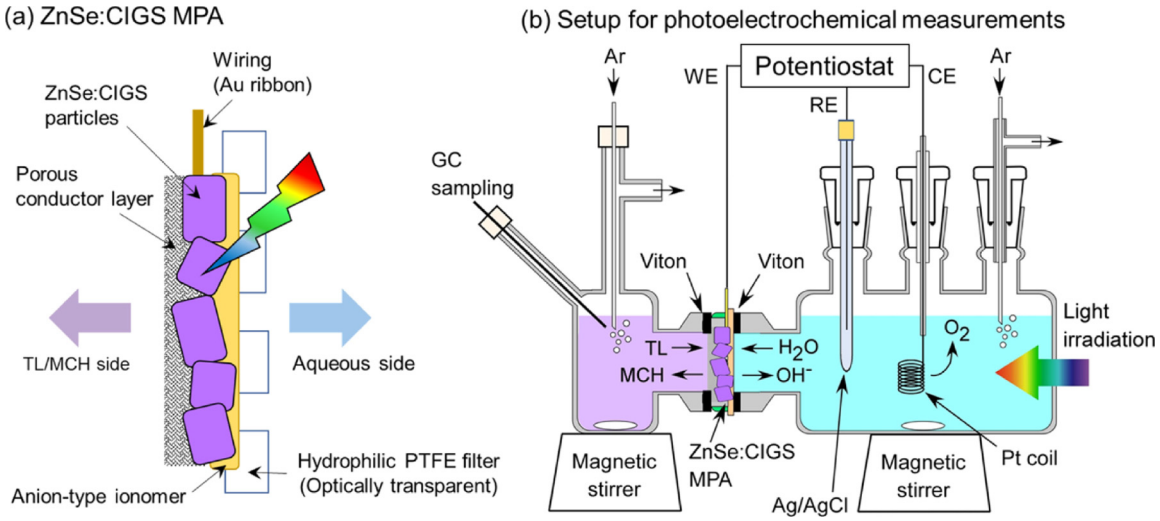

Fig. 10. Schematic drawings of (a) a membrane photocathode assembly (MPA) consisting of a commercially-available membrane filter and self-supported ZnSe:CIGS photocathode prepared by a particle transfer method and (b) a two-chamber PEC cell composed of aqueous and toluene/methylcyclohexane (TL/MCH) chambers separated by the ZnSe:CIGS MPA. Reprinted with permission from Ref. [132]. © 2018, American Chemical Society.

negligible electrochemical activity and light absorption.

3. Ammonia synthesis

The development of the Haber-Bosch Process, which currently accounts for the production of around 174 million tons of ammonia annually, was a landmark achievement of the 20th Century [136]. Over 85 % of the ammonia produced is used in synthetic fertilizers which are credited with the sustenance of around 40 % of the global population. The process involves the reaction of hydrogen with nitrogen in the presence of a promoted iron catalyst and is operated at high pressure (> 100 atm) favoring ammonia formation. Whilst thermodynamically, ammonia synthesis is favored at low reaction temperatures (ΔG°_{f} = -16.2 kJ mol^{-1} at 25 °C), kinetics dictate operation at ca 350–500 °C and elevated pressures are needed to achieve acceptable process yields (Fig. 11). The hydrogen feed for the process is derived from fossil fuel sources such as natural gas. It has been recently estimated that the current operation of industrial ammonia synthesis accounts for ~2.5 % of global fossil fuel-based CO_2 emissions [136]. Furthermore, when considered in its entirety, including the generation of feed streams, the Haber-Bosch Process is believed to be responsible for ~2 % of the world-wide energy consumption [136]. Whilst the industrial scale

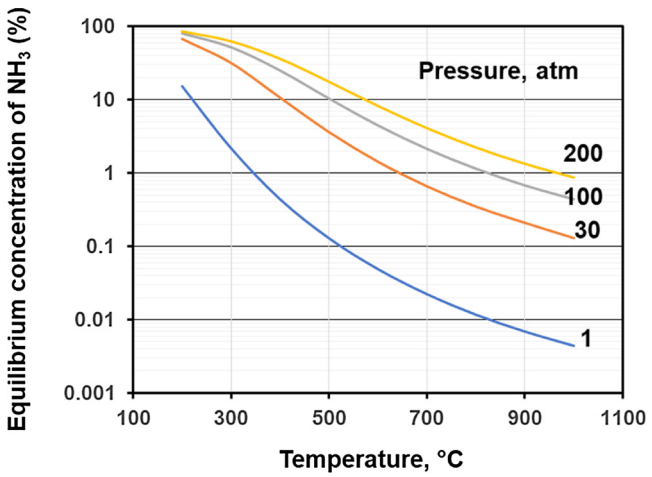

Fig. 11. The percentage of ammonia at equilibrium for a 3/1 H_2/N_2 mixture as a function of temperature and pressure. Data taken from Reference [138].

synthesis has evolved to be a relatively mature technology which is operated on the large scale in highly integrated and very efficient plants, the iron-based catalysts employed continue to be similar to those developed over a century ago. Recently there has been a resurgent interest in the discovery of new catalytic materials due to three, to an extent inter-related, motivations:

(i) The increasing availability of electricity derived from renewable sources such as wind and tidal power, which makes the large-scale, economic and fossil-free generation of hydrogen via water electrolysis an increasingly realistic prospect. In this context, ammonia might also be an appropriate energy storage molecule for intermittent periodic oversupply and peak demands of electricity necessitating reactors which can be started up quickly;
(ii) The increasing interest in the application of ammonia as a fuel. Whilst ammonia synthesis is currently growing at a rate of around 1.5 %–2.0 % per annum [137], its application as a fuel would require a significant growth in the synthesis capacity for which the ability to generate “green ammonia” as detailed in (i) above would be desirable in terms of sustainability and for more localized production;
(iii) Expansion in the ability to produce ammonia at localized smaller-scale facilities which is of potential importance for establishing processes in locations where there is little infrastructure, such as in remote global locations or on farmland for the production of “on-demand” locally derived fertilizer.

All of the above considerations impact upon current, or projected, anthropogenic CO_2 footprints. For example, (ii) is viewed as a replacement for current fossil fuel requirements and indeed there were buses driven on ammonia as fuel operational in Belgium in 1943, and as a partial replacement for the large scale CO_2-intensive production facilities employed today, (iii) offers potential additional savings in offsetting fossil fuel-driven transportation of ammonia-based fertilizers to their points of application. As can be anticipated, heterogeneous catalysis has a potential major role to play in the development of more sustainable localized ammonia production. Here we focus on discussion of potential routes and challenges to improve the energy and CO_2 footprint. The emphasis is on catalyst design in heterogeneous thermal catalytic processes, electrocatalytic, and photocatalytic processes. Although ammonia synthesis is possible with homogeneous catalytic routes [139], this approach will not be discussed in this perspective.

3.1. Thermal catalytic (Haber-Bosch) process

In industrial practice, the predominantly applied catalyst is based on promoted Fe systems which differ only in minor ways from the original formulations. Such formulations include the presence of alumina as a structural promoter along with electronic promoters based upon alkali and alkaline earth metals such as K and Ca [140]. Whilst the system may seem simple, it is indeed more complex and is, for example, enhanced by structural distortion. Fortunately, fundamental surface science studies have underpinned much of the fundamental understanding. The reaction is structure sensitive with the rate-determining N_2 activation step being favored on C7 sites (iron atoms with seven nearest neighbours) associated with surfaces such as the (111) surface plane [141], and only about 5 % of the geometric surface in the industrial catalyst participating in reaction [142]. More recently, a commercial carbon-supported Ru based catalyst has been developed which is about 20 times more active than the commercial iron-based Haber-Bosch catalyst. The higher activity of this catalyst permits less demanding process operational parameters. This catalyst forms the basis of the Kellogg Advanced Ammonia Process (KAAP) which was announced in 1994. The background to the origin of this catalyst is detailed in a very nice overview [143]. A significant challenge in relation to this catalyst was the development of hydrogenation-resistant mesoporous graphitic support. In the Ru system, the B5 site has been identified as being particularly active [144,145]. This site is associated with steps and comprises five Ru atoms. The abundance of these B5 sites is dependent upon catalyst metal dispersion and crystallite morphology and therefore the reaction is strongly structure sensitive with a strong particle size and morphology dependence. Such sites have a maximum occurrence for particle size in the range 1.8–2.5 nm with only (001) and (100) surfaces exposed [146]. Whilst the commercial catalyst uses a carbon-based support, BN (which is isoelectronic with C and which can exist in a graphite as well as a diamond-like structure) has been reported as a very effective and hydrogenation-resistant support [147]. Basic supports such as MgO and Pr_2O_3 are also reported to generate highly active Ru-based catalysts [148].

Mechanistically, the reaction in both the Fe and Ru-based systems is widely believed to be of Langmuir-Hinshelwood form with N_2 dissociation being the rate-determining step. Unlike Fe where *N inhibits the synthesis reaction, in the case of Ru, the reaction is inhibited by adsorbed *H instead [28]. Alkali promoters reduce the effect meaning that the reaction rate is not adversely affected under a high concentration of ammonia as might be the case close to the reactor exit [28].

Of all the chemical elements, Ru exhibits the highest activity. In this context it is interesting to note that Os, the third chemical element in the same group as Fe and Ru, was also recognized to be highly active for ammonia synthesis, particularly in the early work of Haber [149]. In a general context, the catalytic performance of metals for ammonia synthesis has been rationalized on the basis of a scaling relationship by Nørskov and co-workers [150,151], which states that the strength of nitrogen binding on a metal surface is related to ammonia synthesis activity: too weak binding results in difficulties in activating the N_2 molecule, and too strong binding results in slow removal of *N. This explanation results in a Sabatier volcano type relationship, as presented in Fig. 12 [150], which demonstrates that there is an optimal performance as a function of *N binding energy.

For catalysts based on pure metals, this optimum corresponds to Ru. In terms of the discussion above, it is interesting to note the relatively high activities of Ru, Fe and Os. Whilst many studies have addressed the performance of Fe and Ru, the two metals which form the basis of commercial ammonia synthesis catalysts, little attention seems to have been directed towards Os. Originally its scarcity was a concern and it is necessary to exercise care in its handling due to potential toxicity. In a recent DFT based study, the barrier for N_2 activation for Os nanoparticles was determined to be similar to that for Ru nanoparticles, with

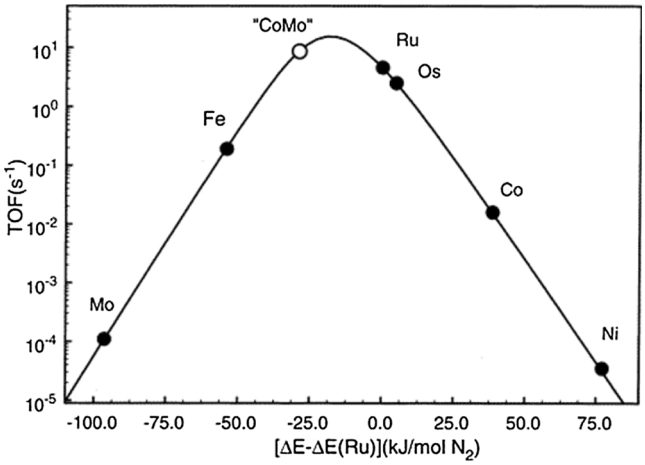

Fig. 12. Calculated turnover frequencies for ammonia synthesis as a function of the adsorption energy of nitrogen (referenced to Ru, 400 °C, 5 MPa, H_2/N_2 3/1 containing 5 % NH_3). Reproduced with permission from C.J.H. Jacobsen, S. Dahl, B.S. Clausen, S. Bahn, A. Logadottir, J.K. Nørskov, J. Amer. Chem. Soc., 123 (2001) 8404–8405 [150]. Copyright 2001 American Chemical Society.

Ru, when existing as 2–4 nm diameter particles, being a better catalyst taking into account activation energy, surface vacancies and density of step sites [151]. Os has also been reported to be very effective for the non-steady state production of NH_3 using sequential nitrogen and hydrogen pulses [152], although this approach does not seem to have been studied further.

Another aspect of the scaling relationship and the volcano plot presented is related to the possibility of tuning catalytic performance by applying appropriate combinations of elements. A specific example of this relates to the catalytic performance of the ternary nitride Co_3Mo_3N which, particularly when promoted with low levels of Cs^+, has been reported to be highly active for ammonia synthesis and competitive with commercial formulations [150,153–158]. The activity of this material has been rationalised on the basis of Fig. 12 with the combination of Mo (which binds nitrogen strongly) with Co (which binds nitrogen weakly) leading to a material that has an activity close to that of the optimal elemental catalyst, Ru [150]. Implicit in this approach is the requirement for structure sensitivity of the Co_3Mo_3N system, with the (111) plane which exposes both Co and Mo being active [150], and no assumed role for the interstitial lattice N in this system beyond ensuring the expression of the active surface lattice plane. Such structure sensitivity has yet to be demonstrated, although there are recent reports that dispersed CoMo catalysts on CeO_2 support are very effective and efficient particularly when considered from the viewpoint of Co and Mo utilization [159,160].

There is recent evidence to suggest that interstitial N may participate in the reaction mechanism in the form of a nitrogen-based Mars-van Krevelen mechanism. The reducibility of Co_3Mo_3N, forming ammonia, was demonstrated with the formation of the previously unreported Co_6Mo_6N phase [161–163]. Isotopic N exchange experiments demonstrated that the lattice N is exchangeable in this system [164] and computational modelling indicated the N vacancy concentration in the Co_3Mo_3N to be potentially significant in the temperature regime of interest for ammonia synthesis [165]. Further modelling has also probed the activation steps for N_2 and H_2 in the system [166] as well as the energy profiles of potential mechanisms [167]. Fig. 13 presents one such mechanism that is energetically favorable. Interestingly, this mechanism is associative in nature, in that there is no N_2 dissociation preceding initial hydrogenation, which is more akin to enzymatic systems. It is also notable that the homomolecular exchange of N_2 (i.e. $^{14}N_2/^{15}N_2$ isotopic scrambling) which can be a probe of N_2 dissociation, was not observed over Co_3Mo_3N at 400 °C [164], although the material catalyzes ammonia synthesis at this temperature. The suggestion of

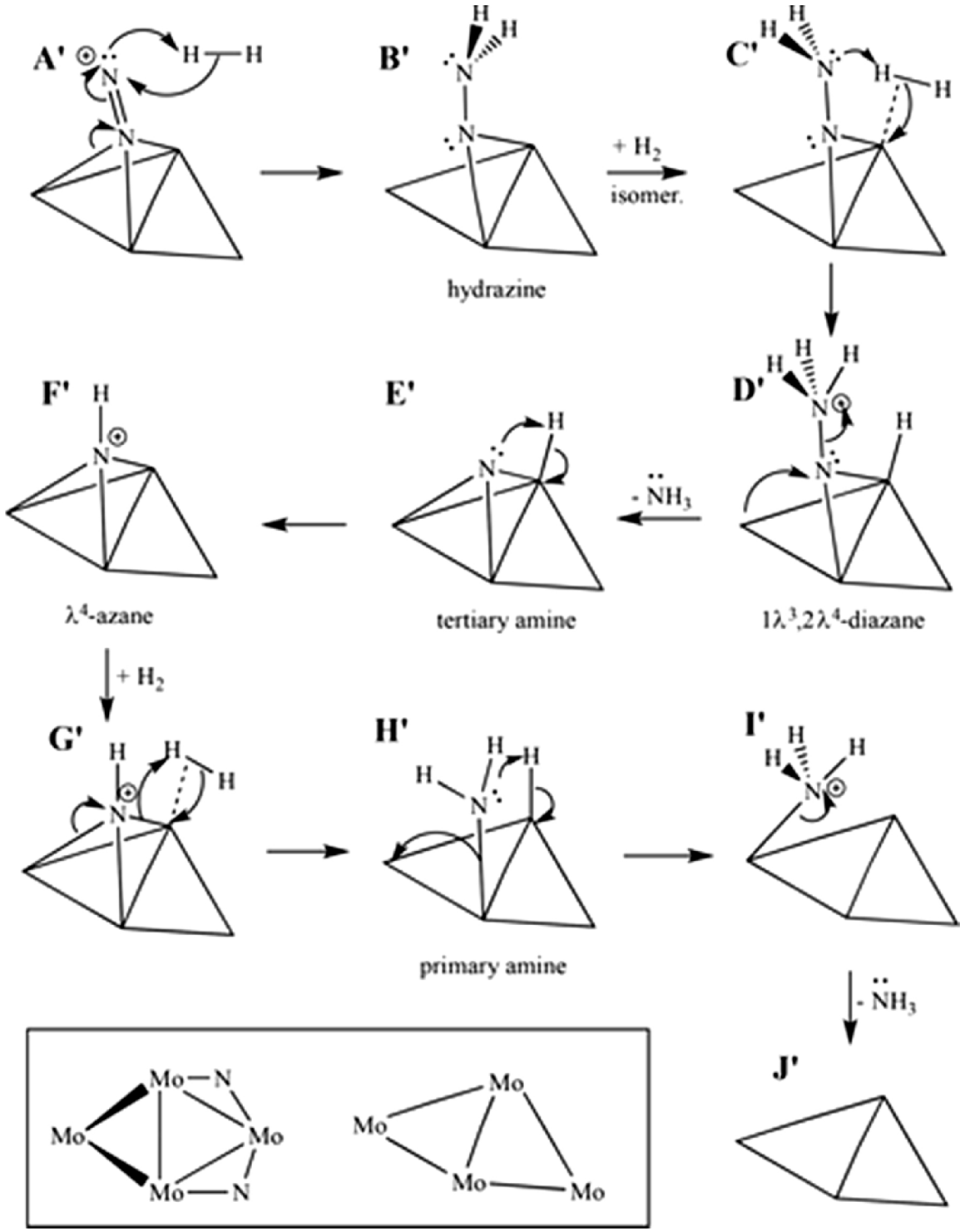

Fig. 13. Possible Mars-van Krevelen/Eley-Rideal ammonia synthesis mechanism with Co_3Mo_3N catalyst. Reproduced from Reference [167]. Copyright 2018 American Chemical Society.

ammonia synthesis occurring via an associative mechanism is rare in the heterogeneous catalytic literature, although it has been proposed as a minor pathway for the Ru catalyst [168]. The link that such a pathway produces with respect to the much slower but ambient condition conversion of N_2 by nitrogenase [169] could be potentially significant in the development of heterogeneous catalysts active at lower reaction temperatures.

It should be noted that there are reports in the literature which propose that the Co_2Mo_3N phase, present as an impurity along with Co_3Mo_3N, is a very active catalyst [170,171]. To date, this has not yet been studied in detail. In terms of ternary nitride catalysts, Ni_2Mo_3N and Fe_3Mo_3N demonstrate high activity [146,156], although they have been less widely investigated than Co_3Mo_3N which generally seems more active. It is possible to rationalize the performance of Ni_2Mo_3N on the basis of Fig. 12. For these nitride systems, the Mars-van Krevelen mechanism may also apply and the lattice nitrogen of Ni_2Mo_3N has been observed to be less reactive than that in Co_3Mo_3N, with the ternary phase $CoNiMo_3N$ being comparable to Ni_2Mo_3N [172]. By

judicious choice of preparation route, it is possible to prepare Ni_2Mo_3N to become comparable in performance to Co_3Mo_3N, which is a significant finding in the context that the nickel-containing material can be more conveniently prepared by treatment of its oxide precursor with ammonia synthesis gas mixture at 700 °C whereas the cobalt material requires an ammonolysis step [172]. The problematic nature of ammonolysis on the large scale is related to heat transfer, which has been documented in the production of binary molybdenum nitrides [173]. A further consideration in relation to the preparation of Ni_2Mo_3N is the difficulty in obtaining a pure phase [172,174]. It is also important to note that misidentification of Ni_2Mo_3N as Ni_3Mo_3N (which has yet to be prepared, although there is precedent of the related Ni_3Mo_3C phase in the literature) occurs fairly frequently in the literature [175] and still continues.

Recent studies have reported hydride and electrides to be new classes of material to serve as a component of ammonia synthesis catalysts. Both TiH_2 and $BaTiO_{2.5}H_{0.5}$ have been demonstrated to be as active as the supported Ru systems [176]. In this context, the application of $BaTiO_{2.5}H_{0.5}$ as a support for Ru, Fe and Co catalysts has been reported to enhance ammonia synthesis rates to the extent that Fe and Co supported on this hydride are more active than Ru/MgO [177]. The hydridic supports are much more active than their perovskite counterparts (Co/$BaTiO_3$ being 400 times less active than Co/$BaTiO_{2.37}H_{0.63}$, and Fe/$BaTiO_3$ 70 times less active than Fe/$BaTiO_{2.35}H_{0.65}$ at 400 °C and 5 MPa). Other studies have demonstrated high activities to be associated with the presence of hydrides [178,179].

There is a series of publications outlining the application of electrides, such as $Ca_2N{:}e^-$ and $[Ca_{24}Al_{28}O_{64}]^{4+}(e^-)_4$, as supports for catalytically active metals [180–188]. The electride supports can enhance the performance of Ru significantly, and the surface reactions of *N and *H become rate determining as opposed to N_2 dissociation. In some electrides, hydride formation has been documented and this results in reduction of hydrogen poisoning of the ammonia synthesis kinetics rather than the generation of an active species. To avoid the activity decline associated with sintering of metal nanoparticles supported on electrides, the interelectride phase LaRuSiH has been prepared and shown to exhibit high activity [188]. In this work, a model based on the following reaction steps and in which hydride ions play a pivotal role was proposed: (i) reversible exchange of H^- with e^-, (ii) N_2 adsorption and dissociation via the hot atom mechanism, (iii) desorption of H facilitated by the heat generated by nitrogen adsorption, and (iv) formation of NH_3 for which its desorption via weakening of the Ru-N bond and the regeneration of the H^- occurs upon further hydrogenation. In the detailed discussion of the reaction mechanism for the LaRuSiH system, the authors stated that the data were also consistent with the Mars-van Krevelen-based associative mechanism which had been previously reported for Co_3Mo_3N [167]. Clearly, further work is necessary to definitively establish the mechanism in operation.

Fig. 12 suggests that Co-based systems would not be expected to be very effective catalysts for ammonia synthesis due to the sub-optimal adsorption energy of nitrogen. However, over the years, a number of studies have documented rather high activities for supported Co and other Co-based materials, such as those presented in Table 2 [60], which include the combination of Co with hydrides and those supported on 12CaO·7AlO-based electrides [189]. For the latter samples, as for the proposals made for Ru, the enhanced ammonia synthesis activity has been ascribed to more facile N_2 activation as a consequence of facilitated electron injection into the supported Co nanoparticles. Related to this suggestion, LaCoSi in which Co was reportedly negatively charged enhanced N_2 activation and shifted the rate-determining step of the reaction to the formation of NH_x species [187].

In addition to activity, a practical catalyst also requires stability. In this context, although Co/CeO_2 was reported to be more active than CoMo/CeO_2 for the first ~25 h on stream, perhaps contrary to the expectation arising from Fig. 12, it exhibited significant deactivation whereas the CoMo system was relatively stable for > 100 h [160]. It has been suggested that the deactivation was due to sintering, which might be mitigated to some extent using a synthetic route employing dopamine [190].

Table 2
The ambient pressure ammonia synthesis rates of various cobalt and other catalysts reported in the literature. Table adapted from reference [189].

Catalyst	Temperature (°C)	Ammonia synthesis rate (μmol h^{-1} g^{-1})	Reference
Co/C12A7:e^-	340	912	[189]
Ru/C12AA7:e^-	340	2290	[189]
Co/CeO_2	340	206	[189]
LaCoSi	400	1250	[187]
Cs-Co_3Mo_3N	400	986	[156]
Co-LiH	350	12000*	[196]

* Rate corresponding to 1.0 MPa reaction pressure.

Whilst not considered from the viewpoint of Co, but rather the stabilization of an unconfirmed enhanced stability rhenium nitride phase, CoRe catalysts are very active for ammonia synthesis [191,192]. Comparable materials comprising FeRe and NiRe were not as effective and, based upon the comparison with rhenium nitride, ammonolysis was employed to prepare materials from their oxidic precursors. The optimum catalyst corresponded to the composition $CoRe_4$ [192]. Subsequently, ammonolysis was replaced by pretreatment with ammonia synthesis gas and again active catalysts were formed [193]. Substituting N_2/H_2 for Ar/H_2 during preparation led to an observed induction period which was also mirrored in a modified homomolecular nitrogen isotopic exchange pattern [193]. Whilst it is tempting to invoke the necessity of a (surface) nitride phase, *in situ* XAS studies demonstrated the pretreatment gas to influence the extent of Co-Re mixing [194]. This illustrates that pretreatment where the formation of active phases through processes such as segregation etc. can play a strong role. This is an aspect which is seldom studied in detail. Cesium-promoted alumina-supported rhenium catalysts have also been reported to be active for ammonia synthesis with some rhenium nitride being present, which is more active than rhenium metal [195]. Whilst cobalt rhenium systems exhibited activities comparable with the more active ammonia synthesis catalysts, they possessed very low surface area (frequently < 0.5 m^2 g^{-1}) and hence had very significant surface area-normalized activity. On this basis, it certainly seems worthwhile to explore the performance of materials comprising highly dispersed CoRe phases.

3.1.1. Opportunities and challenges

Methods to improve an ammonia synthesis catalyst can be based on the conventional mechanistic understanding of the need to balance the activation of N_2 to form *N and the reactivity of this *N atom being limited by the scaling relationship shown in Fig. 12. In this context, attempts to exploit the synergistic combination of alkali and alkaline earth hydrides with transition metals [178] or nitrides [179] have demonstrated success. In such a combination, the hypothesis is that nitrogen activated by the metal/metal nitride is reduced by hydride ions and the resulting species undergo further hydrogenation forming the product and regenerating the active phase. Potentially related to this catalytic cycle is the observation of ammonia synthesis activity for amide-based catalytic materials [197]. The reports of using hydrides and electrides as supports are interesting and worthy of further investigation, especially to improve our understanding of the cause of their effects and the implication on the scaling relationship. Exploring different preparation methods to improve the exposed surfaced area of the active phase is also a recognized direction of research. It should be noted that whilst a number of interesting materials have been reported in the literature, little attention is directed towards prolonged lifetime/accelerated deactivation testing and the stability of performance of catalysts when fed with feedstocks containing impurities, and even less to the practicality of scaling up the preparation and handling of the

materials produced in exploratory tests.

The recent publications of the relevance of the Mars-van Krevelen mechanism to ammonia synthesis [176] offer a new direction that could circumvent scaling limitations and serve as the key to the development of heterogeneous catalysts active under milder reaction conditions. In this context, there is interest in systems based on chemical looping. This approach involves the treatment of a nitride or related material such that ammonia is generated in a stoichiometric reaction involving the nitride following which the nitrogen-depleted material is regenerated such that the cycle can be repeated. In the literature, both metal nitrides [198–204] and imides [205] have been investigated, and ammonia production via hydrogenation of a nitride [206,207] or via hydrolysis of the nitride [198–204] has been reported. In such approaches, the reactivity of lattice nitrogen is an important factor, and theory has been employed to explore the modification of lattice nitrogen reactivity and enhanced ammonia production [166]. Most notably, nitrogen-doped perovskites [208], binary nitrides of magnesium, aluminum, calcium, chromium, manganese, zinc, and molybdenum [201], manganese nitrides [203] and calcium nitride [201] have been investigated for this purpose, as has the hydrolysis of lithium nitride which is of interest due to the nitridation of lithium metal directly with dinitrogen [209]. Whilst it is not strictly conventional catalysis, this approach affords the possibility of producing ammonia under conditions of ambient pressure avoiding potentially limiting scaling relationships. Together with the more conventional heterogeneous catalysis approach, it is an area of increasing interest and is certainly an area worthy of additional attention. The route based upon AlN has recently been discussed from a process orientated viewpoint where a high system efficiency close to 70 % has been reported [210].

It is worthy to note that the Mars-van Krevelen mechanism is increasingly postulated for electrocatalytic ammonia synthesis as well, as discussed in the next section. Likewise, there is an increasing interest to explore associative mechanism of nitrogen activation, akin to nitrogenase routes with electrons taking the place of ATP. At present, the attained productivity is low and there are false results due to contaminations and other artefacts. Nonetheless, they possess rich potential.

The drive to develop more active catalysts to facilitate smaller scale and localized ammonia production is based upon the increasing availability of low cost, sustainably-derived, fossil fuel-free, hydrogen production. Aside from the ever-increasing demand for ammonia for global food production, ammonia increasingly attracts attention as an alternative fuel or energy vector. Such considerations might also drive an expansion of highly centralized large-scale production facilities into areas where none exists currently, such that new processes, not dependent upon the optimized integration currently in place, are desirable. This increased recent interest in ammonia synthesis is reflected in the academic literature and a number of interesting catalytic materials and mechanistic approaches towards ammonia synthesis have been reported recently.

Whilst the impression is sometimes conveyed in some studies that the Haber-Bosch Process is inefficient, it has to be recognized that the process is highly integrated and optimized and that the catalyst employed which, when treated appropriately, is operational for a very long time (> 10 years) and is based on an earth-abundant, non-toxic and cheap element. Furthermore, whilst sometimes desirable from the fundamental point of view when the goal is to generate information on, e.g. lattice component reactivity or the influence of phase interconversion, the applicability of data generated from catalytic tests operated under conditions of ambient pressure to industrial practice needs to be carefully considered. For example, the equilibrium limited ammonia yield at ambient pressure and 400 °C employing 3:1 H_2:N_2, a commonly applied testing regime, is only 0.4 % (Fig. 11). It is an unrealistic reaction regime for genuine application. A further related concern that is seldom addressed is that in industrial practice, reaction mixtures are recycled and contain some ammonia which potentially adversely affects catalytic performance. Aside from these considerations, recent years have witnessed a significant resurgence of interest in the area of ammonia synthesis. A number of exciting developments have been reported and it can be anticipated that further excitement lies ahead. Computational modelling is assuming a more central role [211] and there is increasing recognition of the mutual benefit to be gained through the combination of different approaches to nitrogen activation and the extent to which learning can be transferred between different approaches (e.g. between heterogeneous catalysis, electrocatalysis, photocatalysis and enzymatic catalysis) [212].

3.2. Electrochemical and photocatalytic processes

The production of NH_3 by electrochemical synthesis and other methods has been summarized in several recent reviews [23,138,213,214]. The associated electrochemical methods may be categorized depending on the type of electrolyte, operational temperature, and whether N_2 is directly reduced to NH_3 on the cathode or H_2 is initially generated and then fed to a thermal catalytic process for the conversion of H_2 and N_2 to NH_3. Generally, in electrochemical synthesis, N_2 molecules either are reduced to N^{3-} ions or react with H atoms at the cathode while electrons for the cathodic reactions are extracted from reactants at the anode. The electrochemical synthesis of NH_3 using an aqueous electrolyte solution has rarely been reported because the solubility of N_2 is low and the reaction temperature must be below the boiling point of water. The use of a single-compartment cell supplied with a mixture of N_2 and H_2 or the coexistence of H_2 in the cathode chamber has been shown to possibly increase the resistance of the cathode to oxidation due to O_2 impurity in a feed gas [215]. However, it is preferable to supply pure N_2 and H_2 separately so as to minimize the competitive adsorption of H_2 (or H_2 poisoning) while maximizing the adsorption of inert N_2 on the cathode catalysts. For these reasons, the most common electrochemical cell has a two-compartment design in which the compartments are separated by an electrolyte, such as a proton-conducting polymer membrane, molten salt or solid-state ceramic, depending on the operational temperature (Fig. 14).

In such systems, proton-conducting polymers, molten salts and ceramic membranes may be employed at low ($T < 100$ °C), intermediate (100 °C < T < 500 °C) or high ($T > 500$ °C) temperatures, respectively [23,138,213,214]. In the case of a solid proton-conducting electrolyte, H_2 is oxidized at the anode to give protons, and the resulting electrons are transferred to the cathode through an external circuit, while the protons migrate through the electrolyte to the cathode chamber. Ideally, at the cathode, N_2 reacts with the protons and electrons provided through the electrolyte and electric circuit, respectively. However, it is also possible for the protons to be reduced to H_2 without reacting with N_2, which would reduce the current (or Faradaic) efficiency for NH_3 synthesis to below unity.

Other ionic species can also migrate between the anode and cathode, including nitride ions (N^{3-}) in molten salts containing Li_3N, hydroxide ions (OH-) in molten hydroxides and oxide ions (O^{2-}) in solid ceramic electrolytes [138]. In a system employing a Li_3N-containing molten salt, N^{3-} ions generated by N_2 reduction at the cathode are released into the molten salt electrolyte and migrates to the anode to react with H_2 to produce NH_3. In this case, oxidation of N^{3-} ions to N_2 is an undesirable side reaction. When molten hydroxides and solid ceramic electrolytes are used, N_2 and water are simultaneously fed into the cathode chamber, where N_2 is reduced to NH_3 and ionic species such as OH- and O^{2-} are transferred to the anode chamber and oxidized to O_2. In this scheme, the resulting NH_3 contains water owing to the presence of unreacted feed water. In any case, the rapid migration of ionic species is essential for efficient electrochemical NH_3 production, and higher temperatures are preferable to ensure efficient ionic conduction and kinetic activation for the NH_3 synthesis reaction. However, because the synthesis of NH_3 from H_2 and N_2 is an exothermic reaction,

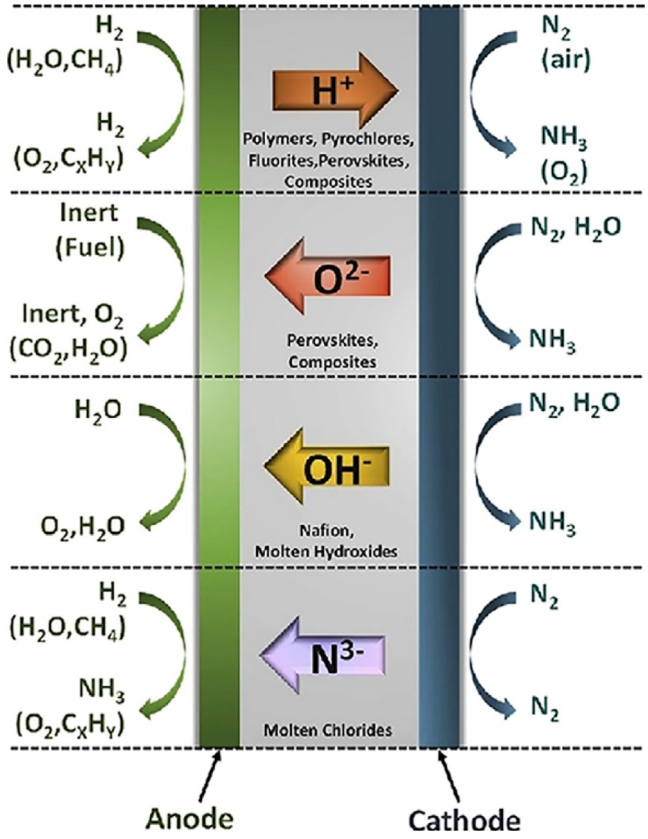

Fig. 14. Schematic depicting the four main strategies (including electrodes and electrolytes) for the electrochemical synthesis of NH_3 from N_2, H_2 and H_2O based on an electricity input (preferably renewable). Reprinted with permission from Ref. [138]. © 2016 Elsevier Inc.

it is also desirable to lower the reaction temperature to obtain a more favorable equilibrium conversion of reactants to NH_3. Therefore, there is a challenging trade-off between kinetics and thermodynamics in electrochemical NH_3 synthesis, similar to the Haber-Bosch process.

Kubota et al. reported dry NH_3 synthesis using electrochemical membrane reactors at a moderate temperature of 250 ^{0}C that balanced the thermodynamics and kinetics of the reaction [216]. The reaction cell was composed of a catalyst that generates ammonia [217], a hydrogen-permeable alloy membrane and a water electrolyzer based on a phosphate electrolyte (Fig. 15). In this system, water is oxidized to O_2 and the resulting protons migrate through a phosphate electrolyte to a Pd-Ag alloy membrane cathode where H_2 is produced. This H_2 is subsequently absorbed by the Pd-Ag alloy membrane and transported to an adjacent NH_3 synthesis catalyst based on $Ru/Cs^+/MgO$. This process involves catalytic reduction of N_2 by H_2 rather than an electrochemical process. Nevertheless, the mechanism is equivalent to electrochemical NH_3 synthesis because it involves electrochemical water splitting and NH_3 synthesis in thermal equilibrium. In an initial study of this system using N_2 and H_2O feed gases at atmospheric pressure, the NH_3 production rates were in the range of 9.0–7.7 $\times$ 10^{-10} mol s^{-1} cm^{-2}, with a current efficiency of 2.6–3.5 % [216,218]. H_2 evolution was found to be a major side reaction that lowered the current efficiency. However, a supply of excess N_2 evidently favored NH_3 synthesis by suppressing the competitive adsorption of H_2 on the Ru catalyst that otherwise prevented the cleavage of the N_2 triple bond. In fact, the reaction order with respect to H_2 was typically negative, although the order was dependent on the catalyst support employed and the activation states during the reaction [28,217]. More recently, the NH_3 formation rate and the current efficiency were improved to 1.24 $\times$ 10^{-8} mol cm^{-2} s^{-1} and 12 %, respectively, by increasing the reaction pressure to 0.7 MPa

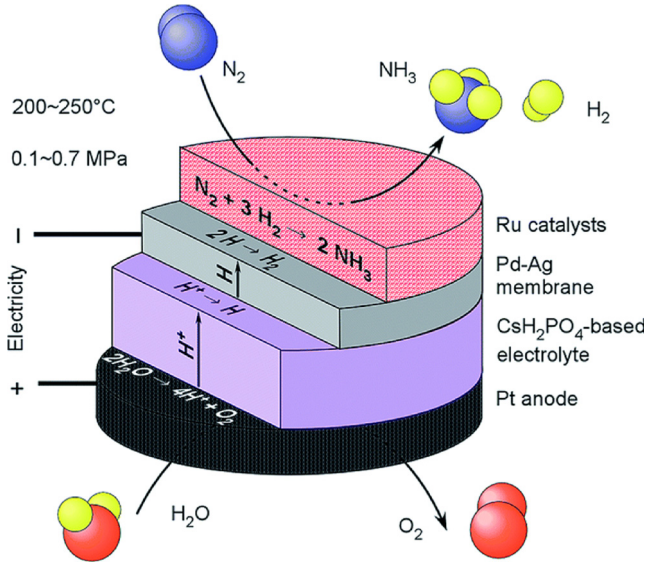

Fig. 15. Schematic showing the concept of a hydrogen-permeable membrane electrochemical reactor for NH_3 synthesis. Reprinted with permission from Ref. [219]. © 2019, The Royal Society of Chemistry.

[219].

Instead of direct reduction of nitrogen molecules, an electrochemical lithium cycling process at intermediate temperatures and ambient pressure was suggested in 2017 (Fig. 16) [220]. LiOH is electrolyzed in a molten bath at 400–450 °C, where ionic Li^+ is reduced into metallic Li on a cathode and OH^- ions are oxidized into water and O_2 on an anode. These electrodes are separated with a porous alumina diffusion barrier to avoid side reactions of reactants and products. Metallic Li is collected and subjected to reaction with molecular N_2 to form Li_3N, which is then hydrolyzed to LiOH to produce NH_3. The net reaction is $2N_2 + 6H_2O \rightarrow 4NH_3 + 3O_2$. This process excels in the current efficiency (88.5 %) because the N_2 reduction reaction is physically and temporally separated from the NH_3 production reaction, which involves H atoms and therefore the opportunity for the competing, nonproductive H_2 evolution reaction. However, an operation voltage greater than 3 V is needed to drive electrolysis of LiOH. This is a major cause of the low energy efficiency (approximately 40 %). In comparison, the energy efficiency of conventional Haber-Bosch processes is estimated to be 56–70 %, depending on the basis used in the calculation [23,211]. A preliminary techno-economic analysis suggests that the cost of an electrochemical lithium cycling process is higher than the existing Haber-Bosch process using an average industrial electricity price ($0.071 kW h^{-1}) [220]. Thus, very low-cost electricity ($0.02 ≈ kWh^{-1} or less) is needed to make this process competitive.

The photocatalytic production of NH_3 from H_2O and N_2 has also been reported and recently reviewed [214,221]. This method was first reported in 1977, using both pristine and Fe-doped TiO_2 photocatalysts under UV irradiation [222]. More recently, a surface-reduced Bi_2MoO_6 photocatalyst was reported that reduced molecular N_2, supplied by bubbling air through water free of sacrificial reagents, to form NH_3 with apparent quantum yields of 0.73 % using 500 nm radiation and 0.25 % for 600 nm radiation [223]. Very recently, Cu-doped TiO_2 nanosheets were found to be effective in fixing N_2 in water under irradiation at wavelengths up to 700 nm, forming NH_3 [224]. In both cases, it was proposed that oxygen vacancies promoted the chemisorption and activation of molecular N_2. In general, there is insufficient information on the overall reaction mechanism because of the lack of analysis of the oxidation products in most experiments. Likewise, the physical and chemical properties of defects such as oxygen vacancies are not fully understood, especially their evolution under reaction conditions, making it difficult to design and control them.

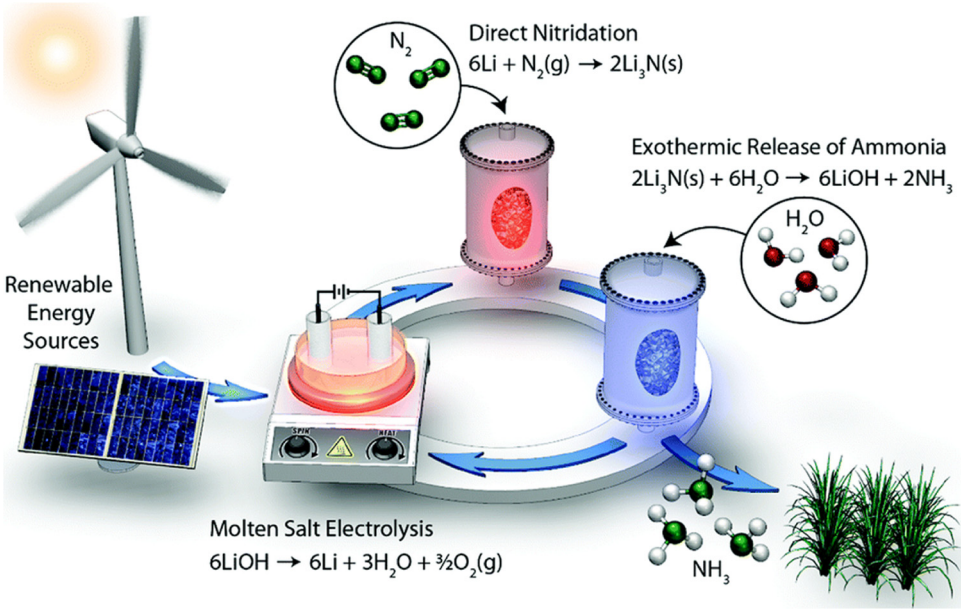

Fig. 16. A scheme demonstrating the concept of sustainable ammonia synthesis based on an electrochemical lithium cycling process. Reprinted with permission from Ref. [220]. © 2017, The Royal Society of Chemistry.

3.3. Opportunities and challenges

For electrochemical production of NH_3, it has been estimated that a Faradaic efficiency > 50 % and an NH_3 production rate > 4–9 × 10^{-7} mol s^{-1} cm^{-2} are required for industrial-scale operations [213]. To date, the reported rates of electrochemical NH_3 synthesis have been mostly on the order of 10^{-8} mol cm^{-2} s^{-1} at best [138,213]. In addition, the Faradaic efficiency tends to decrease with increasing current density in a given system [213], suggesting that the H_2 evolution reaction is responsible for the decline in performance.

For the photocatalytic process, based on past work related to the development of photocatalysts for overall water splitting, the most important requirement is to reduce the density of defects so that active photoexcited electrons and holes can diffuse from the bulk of photocatalytic materials to the surface reaction sites [130]. Defect states tend to trap excited carriers while enhancing charge recombination, which are detrimental to effecting thermodynamic uphill reactions. For ammonia synthesis, the product, NH_3, is also highly soluble in water, whereas the reactant, N_2, is not, which is highly unfavorable on a thermodynamic basis. Consequently, it is a concern that NH_3 may not be able to be accumulated at sufficiently high concentrations to be practical because of its oxidation by photoexcited holes. In fact, it is debatable whether photocatalytic systems capable of efficiently evolving NH_3 can ever be constructed.

Low-temperature activation of the triple bond of molecular N_2 is an interesting but challenging research goal, and a variety of materials and reaction systems have been proposed for this purpose. For electrochemical and photocatalytic processes, it is important to consider the origin of NH_3 during experimental trials, particularly when the NH_3 evolution rate or concentration are very low. NH_3 is the primary pollutant emitted from animal production facilities and from field-applied NH_3-based fertilizers [225]. Thus, the background concentration of NH_3 in the environment varies seasonally and by region, and it has increased over time historically. NH_3 is even found in human breath and can be generated from impurities in the N_2 stream employed in the synthesis system [225]. Furthermore, because it is both polar and basic, NH_3 is readily adsorbed onto, and dissolved into components of the experimental apparatus and test solution, introducing additional variations in the background NH_3 concentration. It is therefore very important to measure the ambient NH_3 concentrations in any aqueous samples to avoid false readings that occur rather frequently [135]. In electrochemical experiments, procedures using open-circuit conditions and employing Ar instead of N_2 should be applied when estimating the background NH_3 concentration, because electrochemical NH_3 production via N_2 reduction does not occur under these circumstances [226]. In addition, it is strongly advisable to perform isotope-labeling experiments to verify the origin of nitrogen atoms in the NH_3 product.

4. Concluding remarks

The two important chemicals focused in this article, NH_3 and H_2O_2, are uniquely interesting in that they can be produced readily by thermal, electrochemical, and photocatalytic techniques starting from the same set of reactants. Thus, they offer the rich possibility of mutually beneficial exchange of expertise and knowledge among the various approaches. To date, there is very limited cross-fertilization of knowledge and ideas across the disciplines. Undoubtedly there are common features among the approaches. For example, for H_2O_2 production, the need to activate O_2 molecule without dissociation into O atoms, the ability to avoid decomposition of the H_2O_2 product and prevent its further oxidation to H_2O and O_2 or hydrogenation are independent of the approach. Likewise, stability of the catalyst and electrocatalyst against leaching is a common concern, and coating appears to be an approach applicable to all processes. What is not yet established is whether these issues share the same or different dependence on catalytic/electrode material properties for the different approaches. In other words, what knowledge is directly transferable? For those that are not, what is the appropriate modification necessary? Is there knowledge that should not be transferred because they are based on different physical principles?

Because less is known about electrochemical or photocatalytic synthesis of NH_3, it is not known if the mechanisms developed for the thermal catalytic approach apply directly, especially requirements of the active sites. This leads to the same question as above: are there general guiding principles that would inform whether certain surface reaction intermediates and their reactions would be common to the different approaches and which would not. Under what circumstances would the reaction step of the highest potential barrier be the same or different? Are the critical steps determining selectivity different and is it possible to predict this a priori?

For the specific reaction of electrochemical and photocatalytic H_2O_2 and NH_3 synthesis, reactions have all been conducted under well-controlled conditions in laboratory experiments, primarily with the aim of increasing the production rate. In some cases, only the detection of intended products is presented. However, at the proof-of-concept stage, the mass balance of reduction and oxidation products should be determined whenever possible, because this information is essential to rule out the involvement of unexpected impurities or unrecognized reaction pathways. The supply and conversion of reactants are also important considerations. These information are necessary to determine the feasibility of scaling up novel production processes and whether such processes are sufficiently energy- and cost-effective to replace current industrial technologies.

Even if H_2O_2 and NH_3 can be accumulated at moderate concentrations, separation, purification and concentration of these products will require additional energy inputs. Therefore, reactors and reaction processes including separation and recycling will be essential for practical applications, similar to the design of facilities for solar hydrogen production by water splitting [130]. Water electrolysis powered by photovoltaics is one of the most efficient means of producing renewable H_2, but this process is thought to be too expensive to supply H_2 at a price acceptable by the market [227]. The supply of H_2 by solar thermochemical reactors using present-day technology [199] will also produce NH_3, but at a cost above the acceptable market price (currently \$0.5 kg^{-1}) [214]. For all these reasons, the development of technology that will radically change the existing chemical industry will require input from the field of chemical engineering.

Declaration of Competing Interest

All authors have declared no financial interest associated with this manuscript.

Acknowledgement

J.S.J. Hargreaves acknowledges support from the EPSRC through grants GR/S87300/01, EP/J018384/1 and EP/L02537X/1 for work in the area of N_2 activation and ammonia synthesis.

T. Hisatomi and K. Domen acknowledge financially support from the Artificial Photosynthesis Project of the New Energy and Industrial Technology Development Organization (NEDO) and a Grant-in-Aid for Scientific Research on Innovative Areas (no. 18H05156) from the Japan Society for the Promotion of Science (JSPS).

Y.-M, Chung and W.-S. Ahn acknowledge support from Basic Science Research Program through the National Research Foundation of Korea (NRF) funded by the Ministry of Education (2016R1D1A3B02006928) and the C1 Gas Refinery Program (2016M3D3A1A01020783) funded by the Ministry of Science and ICT.

H.H. Kung and M.C. Kung acknowledge support from the Institute of Catalysis for Energy Processes, which is supported by the U.S. Department of Energy, Office of science, Basic Energy Sciences under Award Number DOE DE-FG02-03-ER15457.

The authors thank Prof. J. Kubota of Fukuoka University for valuable discussions.

References

[1] Energy-Smart Food for People and Climate, Food and Agriculture Organization of the United Nations, 2011.
[2] The State of Food Security and Nutrition in the World 2017, Building Resilience for Peace and Food Security, FAO, IFAD, UNICEF, WFP and WHO, 2017.
[3] N.G. Shang, P. Papakonstantinou, M. McMullan, M. Chu, A. Stamboulis, A. Potenza, S.S. Dhesi, H. Marchetto, Adv. Funct. Mater. 18 (2008) 3506–3514.
[4] V. Russo, R. Tesser, E. Santacesaria, M. Di Serio, Ind. Eng. Chem. Res. 52 (2013) 1168–1178.
[5] Y. Hu, C. Dong, T. Wang, G. Luo, Chem. Eng. Sci. 187 (2018) 60–66.
[6] Q. Chu, G. He, Y. Xi, P. Wang, H. Yu, R. Liu, H. Zhu, Catal. Commun. 108 (2018) 46–50.
[7] Today in Energy, U.S. Energy Information Administration, https://www.eia.gov/todayinenergy/detail.php?id=18431, (Accessed May 19, 2019).
[8] U.S. Geological Survey, Mineral Commodity Summaries, (February 2019).
[9] R. Ciriminna, L. Albanese, F. Meneguzzo, M. Pagliaro, ChemSusChem 9 (2016) 3374–3381.
[10] N. Liu, F. Luo, H.X. Wu, Y.H. Liu, C. Zhang, J. Chen, Adv. Funct. Mater. 18 (2008) 1518–1525.
[11] Y. Yi, L. Wang, G. Li, H. Guo, Catal. Sci. Technol. 6 (2016) 1593–1610.
[12] R.F. Service, Science (Washington, DC, United States) 361 (2018) 120–123.
[13] C.F. Shih, T. Zhang, J. Li, C. Bai, Joule 2 (2018) 1925–1949.
[14] J.K. Edwards, S.J. Freakley, A.F. Carley, C.J. Kiely, G.J. Hutchings, Acc. Chem. Res. 47 (2014) 845–854.
[15] D.W. Flaherty, ACS Catal. 8 (2018) 1520–1527.
[16] Z.W. Seh, J. Kibsgaard, C.F. Dickens, I. Chorkendorff, J.K. Norskov, T.F. Jaramillo, Science (New York, N.Y.) 355 (2017).
[17] S. Yang, A. Verdaguer-Casadevall, L. Arnarson, L. Silvioli, V. Colic, R. Frydendal, J. Rossmeisl, I. Chorkendorff, I.E.L. Stephens, ACS Catal. 8 (2018) 4064–4081.
[18] A. Yapicioglu, I. Dincer, Renew. Sustain. Energy Rev. 103 (2019) 96–108.
[19] D. Wang, D. Astruc, Chem. Soc. Rev. 46 (2017) 816–854.
[20] K.-i. Tanaka, Y. Yuan, Z. Xie, S.T. Oyama, H. He, Surf. Sci. 679 (2019) 264–272.
[21] H. Tanaka, Y. Nishibayashi, K. Yoshizawa, Acc. Chem. Res. 49 (2016) 987–995.
[22] I.J. McPherson, T. Sudmeier, J. Fellowes, S.C.E. Tsang, Dalton Trans. 48 (2019) 1562–1568.
[23] A.J. Martin, T. Shinagawa, J. Perez-Ramirez, Chemistry 5 (2019) 263–283.
[24] J. Kim, S. Sengodan, S. Kim, O. Kwon, Y. Bu, G. Kim, Renew. Sustain. Energy Rev. 109 (2019) 606–618.
[25] F. Jiao, B. Xu, Adv. Mater. (Weinheim, Germany) 31 (2019) n/a.
[26] J.S.J. Hargreaves, Appl. Petrochem. Res. 4 (2014) 3–10.
[27] A.O. Elnabawy, S. Rangarajan, M. Mavrikakis, J. Catal. 328 (2015) 26–35.
[28] K.-i. Aika, Catal. Today 286 (2017) 14–20.
[29] Nexant, Propylene Oxide - PERP Report, (2003), pp. 12–14 New York.
[30] J.M. Campos-Martin, G. Blanco-Brieva, J.L.G. Fierro, Angew. Chemie Int. Ed. 45 (2006) 6962–6984.
[31] C. Samanta, Appl. Catal. A Gen. 350 (2008) 133–149.
[32] N.M. Wilson, J. Schroder, P. Priyadarshini, D.T. Bregante, S. Kunz, D.W. Flaherty, J. Catal. 368 (2018) 261–274.
[33] I. Huerta, J. Garcia-Serna, M.J. Cocero, J. Supercrit. Fluids 74 (2013) 80–88.
[34] B. Zhou, L.-K. Lee, Catalyst and Process for Direct Catalytic Production of Hydrogen Peroxide, (H_2O_2), Hydrocarbon Technologies, Inc., USA, 2020 Application: US 1998-140265, US 6168775, 2001, pp. 11 pp.
[35] S. Kim, D.-W. Lee, K.-Y. Lee, J. Mol. Catal. A Chem. 391 (2014) 48–54.
[36] Z. Wang, X. Jia, R. Wang, J. Phys. Chem. A 108 (2004) 5424–5430.
[37] P. Tian, L. Ouyang, X. Xu, C. Ao, X. Xu, R. Si, X. Shen, M. Lin, J. Xu, Y.-F. Han, J. Catal. 349 (2017) 30–40.
[38] R. Burch, P.R. Ellis, Appl. Catal. B Environ. 42 (2003) 203–211.
[39] N.M. Wilson, D.W. Flaherty, J. Am. Chem. Soc. 138 (2016) 574–586.
[40] H.C. Ham, G.S. Hwang, J. Han, S.W. Nam, T.H. Lim, J. Phys. Chem. C 113 (2009) 12943–12945.
[41] V.R. Choudhary, C. Samanta, J. Catal. 238 (2006) 28–38.
[42] G.M. Lari, B. Puertolas, M. Shahrokhi, N. Lopez, J. Perez-Ramirez, Angew. Chemie Int. Ed. 56 (2017) 1775–1779.
[43] J.K. Edwards, G.J. Hutchings, Angew. Chemie Int. Ed. 47 (2008) 9192–9198.
[44] R.B. Rankin, J. Greeley, ACS Catal. 2 (2012) 2664–2672.
[45] J.K. Edwards, J. Pritchard, P.J. Miedziak, M. Piccinini, A.F. Carley, Q. He, C.J. Kiely, G.J. Hutchings, Catal. Sci. Technol. 4 (2014) 3244–3250.
[46] N.M. Wilson, P. Priyadarshini, S. Kunz, D.W. Flaherty, J. Catal. 357 (2017) 163–175.
[47] J.K. Edwards, B. Solsona, E. Ntainjua, N, A.F. Carley, A.A. Herzing, C.J. Kiely, G.J. Hutchings, Science (Washington, DC, United States) 323 (2009) 1037–1041.
[48] M.T.M. Koper, J. Electroanal. Chem. 660 (2011) 254–260.
[49] V. Viswanathan, A. Hansen Heine, J. Rossmeisl, K. Norskov Jens, J. Phys. Chem. Lett. 3 (2012) 2948–2951.
[50] X. Shi, S. Siahrostami, P. Chakthranont, F. Jaramillo Thomas, X. Zheng, K. Norskov Jens, X. Shi, Y. Zhang, X. Zheng, G.-L. Li, F. Studt, K. Norskov Jens, G.-L. Li, Y. Zhang, F. Studt, F. Studt, Nat. Commun. 8 (2017) 701.
[51] S. Maity, M. Eswaramoorthy, J. Mater. Chem. A Mater. Energy Sustain. 4 (2016) 3233–3237.
[52] F. Li, Q. Shao, M. Hu, Y. Chen, X. Huang, ACS Catal. 8 (2018) 3418–3423.
[53] S. Wang, K. Gao, W. Li, J. Zhang, Appl. Catal. A: Gen. 531 (2017) 89–95.
[54] S.J. Freakley, Q. He, J.H. Harrhy, L. Lu, D.A. Crole, D.J. Morgan, E.N. Ntainjua, J.K. Edwards, A.F. Carley, A.Y. Borisevich, C.J. Kiely, G.J. Hutchings, Science (Washington, DC, United States) 351 (2016) 965–968.
[55] J.K. Edwards, B.E. Solsona, P. Landon, A.F. Carley, A. Herzing, C.J. Kiely, G.J. Hutchings, J. Catal. 236 (2005) 69–79.
[56] J.K. Edwards, A.F. Carley, A.A. Herzing, C.J. Kiely, G.J. Hutchings, Faraday Discuss. 138 (2008) 225–239.
[57] Y.-M. Chung, Y.-T. Kwon, T.J. Kim, S.-H. Oh, C.-S.L. Lee, Chem. Commun. 47 (2011) 5705–5707.
[58] J. Kim, Y.-M. Chung, S.M. Kang, C.H. Choi, B.Y. Kim, Y.T. Kwon, T.J. Kim, S.H. Oh, C.S. Lee, ACS Catal. 2 (2012) 1042–1048.
[59] I. Yamanaka, J. Jpn. Pet. Inst. 57 (2014) 237–250.
[60] K. Otsuka, I. Yamanaka, Electrochim. Acta 35 (1990) 319–322.
[61] I. Yamanaka, S. Tazawa, T. Murayama, R. Ichihashi, N. Hanaizumi, ChemSusChem 1 (2008) 988–990.
[62] T. Murayama, S. Tazawa, S. Takenaka, I. Yamanaka, Catal. Today 164 (2011) 163–168.

[63] T. Iwasaki, Y. Masuda, H. Ogihara, I. Yamanaka, Electrocatalysis 9 (2018) 236–242.
[64] W. Eul, A. Moeller, N. Steiner, Kirk-Othmer Encyclopedia of Chemical Technology, First published: 17 August Copyright John Wiley & Sons, Inc., 2001, https://doi-org.turing.library.northwestern.edu/10.1002/0471238961.0825041808051919.a01.pub2.
[65] X. Liang, Z. Mi, Y. Wang, L. Wang, X. Zhang, T. Liu, Chem. Eng. Technol. 27 (2004) 176–180.
[66] T. Nishimi, T. Kamachi, K. Kato, T. Kato, K. Yoshizawa, Eur. J. Org. Chem. 2011 (2011) 4113–4120 S4113/4111-S4113/4136.
[67] T. Nishimura, N. Kakiuchi, T. Onoue, K. Ohe, S. Uemura, Perkin 1 (2000) 1915–1918.
[68] R. Bortolo, D. Bianchi, R. D'Aloisio, C. Querci, M. Ricci, J. Mol. Catal. A Chem. 153 (2000) 25–29.
[69] L.-Y. Wang, J. Li, Y. Lv, H.-Y. Zhang, S. Gao, J. Organomet. Chem. 696 (2011) 3257–3263.
[70] B.N. Zope, D.D. Hibbitts, M. Neurock, R.J. Davis, Science (Washington, DC, United States) 330 (2010) 74–78.
[71] J. Jiang, S.M. Oxford, B. Fu, M.C. Kung, H.H. Kung, J. Ma, Chem. Commun. (Cambridge, United Kingdom) 46 (2010) 3791–3793.
[72] W.C. Ketchie, M. Murayama, R.J. Davis, Top. Catal. 44 (2007) 307–317.
[73] M.M. Konnick, B.A. Gandhi, I.A. Guzei, S.S. Stahl, Angew. Chemie Int. Ed. 45 (2006) 2904–2907.
[74] M.M. Konnick, S.S. Stahl, J. Am. Chem. Soc. 130 (2008) 5753–5762.
[75] G. Meier, T. Braun, Angew. Chemie Int. Ed. 51 (2012) 12564–12569.
[76] M.C. Kung, H.H. Kung, Chin. J. Catal. (2019) accepted for publication.
[77] R.A. Sidik, A.B. Anderson, J. Electroanal. Chem. 528 (2002) 69–76.
[78] W.A. Donald, R.D. Leib, J.T. O'Brien, E.R. Williams, Chem. Eur. J. 15 (2009) 5926–5934.
[79] C. Samanta, V.R. Choudhary, Appl. Catal. A: General 330 (2007) 23–32.
[80] G. Gallina, J. García-Serna, T.O. Salmi, P. Canu, P. Biasi, Ind. Eng. Chem. Res. 56 (2017) 13367–13378.
[81] E. Ntainjua, N, J.K. Edwards, A.F. Carley, J.A. Lopez-Sanchez, J.A. Moulijn, A.A. Herzing, C.J. Kiely, G.J. Hutchings, Green Chem. 10 (2008) 1162–1169.
[82] N.M. Wilson, D.T. Bregante, P. Priyadarshini, D.W. Flaherty, Catalysis 29 (2017) 122–212.
[83] S. Yook, H.C. Kwon, Y.G. Kim, W. Choi, M. Choi, ACS Sustain. Chem. Eng. 5 (2017) 1208–1216.
[84] R. Arrigo, M.E. Schuster, S. Abate, G. Giorgianni, G. Centi, S. Perathoner, S. Wrabetz, V. Pfeifer, M. Antonietti, R. Schlögl, ACS Catal. 6 (2016) 6959–6966.
[85] N. E.N, M. Piccinini, J.C. Pritchard, J.K. Edwards, A.F. Carley, J.A. Moulijn, G.J. Hutchings, ChemSusChem 2 (2009) 575–580.
[86] S. Lee, H. Jeong, Y.-M. Chung, J. Catal. 365 (2018) 125–137.
[87] B. Hu, W. Deng, R. Li, Q. Zhang, Y. Wang, F. Delplanque-Janssens, D. Paul, F. Desmedt, P. Miquel, J. Catal. 319 (2014) 15–26.
[88] G. Blanco-Brieva, E. Cano-Serrano, J.M. Campos-Martin, J.L.G. Fierro, Chem. Commun. (2004) 1184–1185.
[89] S. Park, J. Lee, J.H. Song, T.J. Kim, Y.-M. Chung, S.H. Oh, I.K. Song, J. Mol. Catal. A Chem. 363–364 (2012) 230–236.
[90] S. Park, J.H. Choi, T.J.K. Kim, Y.-M. Chung, S.H. Oh, I.K. Song, J. Mol. Catal. A Chem. 353–354 (2012) 37–43.
[91] Y.-M. Chung, Y.-R. Lee, W.-S. Ahn, Bull. Korean Chem. Soc. 36 (2015) 1378–1383.
[92] M.C. Wasson, C.T. Buru, Z. Chen, T. Islamoglu, O.K. Farha, Appl. Catal. A Gen. 586 (2019) 117214.
[93] Y.-M. Chung, H.Y. Kim, W.S. Ahn, Catal. Lett. 144 (2014) 817–824.
[94] S. Yook, H. Shin, H. Kim, M. Choi, ChemCatChem 6 (2014) 2836–2842.
[95] A. Santos, P. Yustos, A. Quintanilla, F. Garcia-Ochoa, J.A. Casas, J.J. Rodriguez, Environ. Sci. Technol. 38 (2004) 133–138.
[96] Y. Yan, S. Jiang, H. Zhang, RSC Adv. 6 (2016) 3850–3859.
[97] C. Su, X. Duan, J. Miao, Y. Zhong, W. Zhou, S. Wang, Z. Shao, ACS Catal. 7 (2017) 388–397.
[98] X. Pang, Y. Guo, Y. Zhang, B. Xu, F. Qi, Chem. Eng. J. (Amsterdam, Netherlands) 304 (2016) 897–907.
[99] Y. Du, W. Ma, P. Liu, B. Zou, J. Ma, J. Hazard. Mater. 308 (2016) 58–66.
[100] M. Ferentz, M.V. Landau, R. Vidruk, M. Herskowitz, Catal. Today 241 (2015) 63–72.
[101] L. Qian, Z. Wang, E.V. Beletskiy, J. Liu, H.J. dos Santos, T. Li, Md.C. Rangel, M.C. Kung, H.H. Kung, Nat. Commun. 8 (2017) 14881.
[102] B.J. O'Neill, D.H.K. Jackson, A.J. Crisci, C.A. Farberow, F. Shi, A.C. Alba-Rubio, J. Lu, P.J. Dietrich, X. Gu, C.L. Marshall, P.C. Stair, J.W. Elam, J.T. Miller, F.H. Ribeiro, P.M. Voyles, J. Greeley, M. Mavrikakis, S.L. Scott, T.F. Kuech, J.A. Dumesic, Angew. Chem. Int. Ed. 52 (2013) 13808–13812.
[103] H. Chen, K. Shen, Q. Mao, J. Chen, Y. Li, ACS Catal. 8 (2018) 1417–1426.
[104] W. Zhan, Q. He, X. Liu, Y. Guo, Y. Wang, L. Wang, Y. Guo, A.Y. Borisevich, J. Zhang, G. Lu, S. Dai, J. Am. Chem. Soc. 138 (2016) 16130–16139.
[105] O.A. Abdelrahman, H.Y. Luo, A. Heyden, Y. Roman-Leshkov, J.Q. Bond, J. Catal. 329 (2015) 10–21.
[106] Q. Yang, H. Choi, S.R. Al-Abed, D.D. Dionysiou, Appl. Catal. B Environ. 88 (2009) 462–469.
[107] R.M. Ravenelle, J.R. Copeland, W.-G. Kim, J.C. Crittenden, C. Sievers, ACS Catal. 1 (2011) 552–561.
[108] L. Zhang, K. Chen, B. Chen, J.L. White, D.E. Resasco, J. Am. Chem. Soc. 137 (2015) 11810–11819.
[109] M.W. Hahn, J.R. Copeland, A.H. van Pelt, C. Sievers, ChemSusChem 6 (2013) 2304–2315.
[110] H.N. Pham, A.E. Anderson, R.L. Johnson, T.J. Schwartz, B.J. O'Neill, P. Duan, K. Schmidt-Rohr, J.A. Dumesic, A.K. Datye, ACS Catal. 5 (2015) 4546–4555.
[111] S. Abate, R. Arrigo, M.E. Schuster, S. Perathoner, G. Centi, A. Villa, D. su, R. Schlögl, Catal. Today 157 (2010) 280–285.
[112] A. Plauck, E.E. Stangland, J.A. Dumesic, M. Mavrikakis, Proc. Natl. Acad. Sci. 113 (2016) E1973–E1982.
[113] A. Fujishima, X. Zhang, D.A. Tryk, Surf. Sci. Rep. 63 (2008) 515–582.
[114] Y. Shiraishi, S. Kanazawa, Y. Sugano, D. Tsukamoto, H. Sakamoto, S. Ichikawa, T. Hirai, ACS Catal. 4 (2014) 774–780.
[115] Y. Shiraishi, S. Kanazawa, Y. Kofuji, H. Sakamoto, S. Ichikawa, S. Tanaka, T. Hirai, Angew. Chemie Int. Ed. 53 (2014) 13454–13459.
[116] Y. Kofuji, Y. Isobe, Y. Shiraishi, H. Sakamoto, S. Tanaka, S. Ichikawa, T. Hirai, J. Am. Chem. Soc. 138 (2016) 10019–10025.
[117] Y. Kofuji, Y. Isobe, Y. Shiraishi, H. Sakamoto, S. Ichikawa, S. Tanaka, T. Hirai, ChemCatChem 10 (2018) 2070–2077.
[118] Y. Kofuji, S. Ohkita, Y. Shiraishi, H. Sakamoto, S. Tanaka, S. Ichikawa, T. Hirai, ACS Catal. 6 (2016) 7021–7029.
[119] Y. Kofuji, S. Ohkita, Y. Shiraishi, H. Sakamoto, S. Ichikawa, S. Tanaka, T. Hirai, ACS Sustain. Chem. Eng. 5 (2017) 6478–6485.
[120] H. Hirakawa, S. Shiota, Y. Shiraishi, H. Sakamoto, S. Ichikawa, T. Hirai, ACS Catal. 6 (2016) 4976–4982.
[121] K. Fuku, K. Sayama, Chem. Commun. (Cambridge, United Kingdom) 52 (2016) 5406–5409.
[122] D.E. Richardson, H. Yao, K.M. Frank, D.A. Bennett, J. Am. Chem. Soc. 122 (2000) 1729–1739.
[123] K. Fuku, Y. Miyase, Y. Miseki, T. Gunji, K. Sayama, ChemistrySelect 1 (2016) 5721–5726.
[124] K. Fuku, Y. Miyase, Y. Miseki, T. Gunji, K. Sayama, RSC Adv. 7 (2017) 47619–47623.
[125] Y. Miyase, S. Takasugi, S. Iguchi, Y. Miseki, T. Gunji, K. Sasaki, E. Fujita, K. Sayama, Sustain. Energy Fuels 2 (2018) 1621–1629.
[126] K. Fuku, Y. Miyase, Y. Miseki, T. Funaki, T. Gunji, K. Sayama, Chem. Asian J. 12 (2017) 1111–1119.
[127] T. Setoyama, T. Takewaki, K. Domen, T. Tatsumi, Faraday Discuss. 198 (2017) 509–527.
[128] K. Sayama, ACS Energy Lett. 3 (2018) 1093–1101.
[129] D.E. Scaife, Sol. Energy 25 (1980) 41–54.
[130] T. Hisatomi, K. Domen, Nat. Catal. 2 (2019) 387–399.
[131] T. Minegishi, N. Nishimura, J. Kubota, K. Domen, Chem. Sci. 4 (2013) 1120–1124.
[132] Y. Kageshima, T. Minegishi, S. Sugisaki, Y. Goto, H. Kaneko, M. Nakabayashi, N. Shibata, K. Domen, ACS Appl. Mater. Interfaces 10 (2018) 44396–44402.
[133] T. Takata, C. Pan, M. Nakabayashi, N. Shibata, K. Domen, J. Am. Chem. Soc. 137 (2015) 9627–9634.
[134] C. Pan, T. Takata, M. Nakabayashi, T. Matsumoto, N. Shibata, Y. Ikuhara, K. Domen, Angew. Chemie Int. Ed. 54 (2015) 2955–2959.
[135] H. Dotan, K. Sivula, M. Gratzel, A. Rothschild, S.C. Warren, Energy Environ. Sci. 4 (2011) 958–964.
[136] P.H. Pfromm, J. Renew. Sustain. Energy 9 (2017) 034702/034701-034702/034711.
[137] https://ihsmarkit.com/products/ammonia-chemical-economics-handbook.html, (Accessed 18th January 2019).
[138] V. Kyriakou, I. Garagounis, E. Vasileiou, A. Vourros, M. Stoukides, Catal. Today 286 (2017) 2–13.
[139] J. Sgrignani, D. Franco, A. Magistrato, Molecules 16 (2011) 442–465.
[140] T. Rayment, R. Schlögl, J.M. Thomas, G. Ertl, Nature (London, United Kingdom) 315 (1985) 311–313.
[141] D.R. Strongin, J. Carrazza, S.R. Bare, G.A. Somorjai, J. Catal. 103 (1987) 213–215.
[142] R. Schlögl, Angew. Chemie Int. Ed. 42 (2003) 2004–2008.
[143] D.E. Brown, T. Edmonds, R.W. Joyner, J.J. McCarroll, S.R. Tennison, Catal. Lett. 144 (2014) 545–552.
[144] S. Dahl, A. Logadottir, R.C. Egeberg, J.H. Larsen, I. Chorkendorff, E. Törnqvist, J.K. Nørskov, Phys. Rev. Lett. 83 (1999) 1814–1817.
[145] S. Shetty, A.P.J. Jansen, R.A. van Santen, J. Phys. Chem. C 112 (2008) 17768–17771.
[146] C.J.H. Jacobsen, S. Dahl, P.L. Hansen, E. Törnqvist, L. Jensen, H. Topsøe, D.V. Prip, P.B. Moenshaug, I. Chorkendorff, J. Mol. Catal. A Chem. 163 (2000) 19–26.
[147] C.J.H. Jacobsen, J. Catal. 200 (2001) 1–3.
[148] K. Sato, K. Imamura, Y. Kawano, S.-i. Miyahara, T. Yamamoto, S. Matsumura, K. Nagaoka, Chem. Sci. 8 (2017) 674–679.
[149] F. Haber, The Synthesis of Ammonia From Its Elements, Nobel Prize Lecture (Accessed 15th January 2019), (1918) https://www.nobelprize.org/uploads/2018/06/haber-lecture.pdf.
[150] C.J.H. Jacobsen, S. Dahl, B.S. Clausen, S. Bahn, A. Logadottir, J.K. Nørskov, J. Am. Chem. Soc. 123 (2001) 8404–8405.
[151] A. Ishikawa, T. Doi, H. Nakai, J. Catal. 357 (2017) 213–222.
[152] G. Rambeau, A. Jorti, H. Amariglio, Appl. Catal. 3 (1982) 273–282.
[153] R. Kojima, K.-I. Aika, Chem. Lett. (2000) 514–515.
[154] R. Kojima, K.-I. Aika, Appl. Catal. A Gen. 219 (2001) 157–170.
[155] R. Kojima, K.-I. Aika, Appl. Catal. A Gen. 218 (2001) 121–128.
[156] R. Kojima, K.-I. Aika, Appl. Catal. A Gen. 215 (2001) 149–160.
[157] C.J.H. Jacobsen, Chem. Commun. (Cambridge) (2000) 1057–1058.
[158] A. Boisen, S. Dahl, C.J.H. Jacobsen, J. Catal. 208 (2002) 180–186.
[159] Y. Tsuji, M. Kitano, K. Kishida, M. Sasase, T. Yokoyama, M. Hara, H. Hosono, Chem. Commun. (Cambridge, United Kingdom) 52 (2016) 14369–14372.
[160] Y. Tsuji, K. Ogasawara, M. Kitano, K. Kishida, H. Abe, Y. Niwa, T. Yokoyama, M. Hara, H. Hosono, J. Catal. 364 (2018) 31–39.

[161] D. McKay, D.H. Gregory, J.S.J. Hargreaves, S.M. Hunter, X. Sun, Chem. Commun. (Cambridge, United Kingdom) (2007) 3051–3053.
[162] S.M. Hunter, D. McKay, R.I. Smith, J.S.J. Hargreaves, D.H. Gregory, Chem. Mater. 22 (2010) 2898–2907.
[163] D.H. Gregory, J.S.J. Hargreaves, S.M. Hunter, Catal. Lett. 141 (2011) 22–26.
[164] S.M. Hunter, D.H. Gregory, J.S.J. Hargreaves, M. Richard, D. Duprez, N. Bion, ACS Catal. 3 (2013) 1719–1725.
[165] C.D. Zeinalipour-Yazdi, J.S.J. Hargreaves, C.R.A. Catlow, J. Phys. Chem. C 119 (2015) 28368–28376.
[166] C.D. Zeinalipour-Yazdi, J.S.J. Hargreaves, C.R.A. Catlow, J. Phys. Chem. C 120 (2016) 21390–21398.
[167] C.D. Zeinalipour-Yazdi, J.S.J. Hargreaves, C.R.A. Catlow, J. Phys. Chem. C 122 (2018) 6078–6082.
[168] A.L. Garden, E. Skulason, J. Phys. Chem. C 119 (2015) 26554–26559.
[169] B.M. Hoffman, D. Lukoyanov, Z.-Y. Yang, D.R. Dean, L.C. Seefeldt, Chem. Rev. (Washington, DC, United States) 114 (2014) 4041–4062.
[170] D. Moszynski, P. Adamski, M. Nadziejko, A. Komorowska, A. Sarnecki, Chem. Pap. 72 (2018) 425–430.
[171] P. Adamski, D. Moszynski, M. Nadziejko, A. Komorowska, A. Sarnecki, A. Albrecht, Chem. Pap. 73 (2019) 851–859.
[172] N. Bion, F. Can, J. Cook, J.S.J. Hargreaves, A.L. Hector, W. Levason, A.R. McFarlane, M. Richard, K. Sardar, Appl. Catal. A Gen. 504 (2015) 44–50.
[173] R.S. Wise, E.J. Markel, J. Catal. 145 (1994) 335–343.
[174] S. Alconchel, F. Sapina, D. Beltrán, A. Beltrán, J. Mater. Chem. 8 (1998) 1901–1909.
[175] J.O. Conway, T.J. Prior, J. Alloys Compd. 774 (2019) 69–74.
[176] Y. Kobayashi, Y. Tang, T. Kageyama, H. Yamashita, N. Masuda, S. Hosokawa, H. Kageyama, J. Am. Chem. Soc. 139 (2017) 18240–18246.
[177] Y. Tang, Y. Kobayashi, N. Masuda, Y. Uchida, H. Okamoto, T. Kageyama, S. Hosokawa, F. Loyer, K. Mitsuhara, K. Yamanaka, Y. Tamenori, C. Tassel, T. Yamamoto, T. Tanaka, H. Kageyama, Adv. Energy Mater. 8 (2018) 1801772.
[178] W. Gao, P. Wang, J. Guo, F. Chang, T. He, Q. Wang, G. Wu, P. Chen, ACS Catal. 7 (2017) 3654–3661.
[179] F. Chang, Y. Guan, X. Chang, J. Guo, P. Wang, W. Gao, G. Wu, J. Zheng, X. Li, P. Chen, J. Am. Chem. Soc. (2018) Ahead of Print.
[180] Y. Kobayashi, M. Kitano, S. Kawamura, T. Yokoyama, H. Hosono, Catal. Sci. Technol. 7 (2017) 47–50.
[181] M. Hara, M. Kitano, H. Hosono, ACS Catal. 7 (2017) 2313–2324.
[182] Y. Inoue, M. Kitano, S.-W. Kim, T. Yokoyama, M. Hara, H. Hosono, ACS Catal. 4 (2014) 674–680.
[183] F. Hayashi, M. Kitano, T. Yokoyama, M. Hara, H. Hosono, ChemCatChem 6 (2014) 1317–1323.
[184] M. Kitano, S. Kanbara, Y. Inoue, N. Kuganathan, P.V. Sushko, T. Yokoyama, M. Hara, H. Hosono, Nat. Commun. 6 (2015) 6731.
[185] S. Kanbara, M. Kitano, Y. Inoue, T. Yokoyama, M. Hara, H. Hosono, J. Am. Chem. Soc. 137 (2015) 14517–14524.
[186] M. Kitano, Y. Inoue, H. Ishikawa, K. Yamagata, T. Nakao, T. Tada, S. Matsuishi, T. Yokoyama, M. Hara, H. Hosono, Chem. Sci. 7 (2016) 4036–4043.
[187] Y. Gong, J. Wu, M. Kitano, J. Wang, T.-N. Ye, J. Li, Y. Kobayashi, K. Kishida, H. Abe, Y. Niwa, H. Yang, T. Tada, H. Hosono, Nat. Catal. 1 (2018) 178–185.
[188] J. Wu, J. Li, Y. Gong, M. Kitano, T. Inoshita, H. Hosono, Angew. Chemie Int. Ed. 58 (2019) 825–829.
[189] Y. Inoue, M. Kitano, M. Tokunari, T. Taniguchi, K. Ooya, H. Abe, Y. Niwa, M. Sasase, M. Hara, H. Hosono, ACS Catal. 9 (2019) 1670–1679.
[190] X. Wang, L. Li, T. Zhang, B. Lin, J. Ni, C.-T. Au, L. Jiang, Chem. Commun. (Cambridge, United Kingdom) 55 (2019) 474–477.
[191] R. Kojima, K.-I. Aika, Chem. Lett. (2000) 912–913.
[192] R. Kojima, K.-I. Aika, Appl. Catal. A Gen. 209 (2001) 317–325.
[193] K. McAulay, J.S.J. Hargreaves, A.R. McFarlane, D.J. Price, N.A. Spencer, N. Bion, F. Can, M. Richard, H.F. Greer, W.Z. Zhou, Catal. Commun. 68 (2015) 53–57.
[194] K. Mathisen, K.G. Kirste, J.S.J. Hargreaves, S. Laassiri, K. McAulay, A.R. McFarlane, N.A. Spencer, Top. Catal. 61 (2018) 225–239.
[195] R. Kojima, H. Enomoto, M. Muhler, K.-i. Aika, Appl. Catal. A Gen. 246 (2003) 311–322.
[196] P. Wang, F. Chang, W. Gao, J. Guo, G. Wu, T. He, P. Chen, Nat. Chem. 9 (2017) 64–70.
[197] M. Kitano, Y. Inoue, M. Sasase, K. Kishida, Y. Kobayashi, K. Nishiyama, T. Tada, S. Kawamura, T. Yokoyama, M. Hara, H. Hosono, Angew. Chemie Int. Ed. 57 (2018) 2648–2652.
[198] R. Michalsky, P.H. Pfromm, Sol. Energy 85 (2011) 2642–2654.
[199] R. Michalsky, B.J. Parman, V. Amanor-Boadu, P.H. Pfromm, Energy (Oxford, United Kingdom) 42 (2012) 251–260.
[200] R. Michalsky, P.H. Pfromm, AIChE J. 58 (2012) 3203–3213.
[201] R. Michalsky, P.H. Pfromm, J. Phys. Chem. C 116 (2012) 23243–23251.
[202] R. Michalsky, A.M. Avram, B.A. Peterson, P.H. Pfromm, A.A. Peterson, Chem. Sci. 6 (2015) 3965–3974.
[203] R. Michalsky, A. Steinfeld, H. Pfromm Peter, Interface Focus 5 (2015) 20140084.
[204] N. Shan, V. Chikan, P. Pfromm, B. Liu, J. Phys. Chem. C 122 (2018) 6109–6116.
[205] W. Gao, J. Guo, P. Wang, Q. Wang, F. Chang, Q. Pei, W. Zhang, L. Liu, P. Chen, Nat. Energy 3 (2018) 1067–1075.
[206] S. Laassiri, C.D. Zeinalipour-Yazdi, C.R.A. Catlow, J.S.J. Hargreaves, Appl. Catal. B Envion. 223 (2018) 60–66.
[207] S. Laassiri, C.D. Zeinalipour-Yazdi, C.R.A. Catlow, J.S.J. Hargreaves, Catal. Today 286 (2017) 147–154.
[208] R. Michalsky, A. Steinfeld, Catal. Today 286 (2017) 124–130.
[209] A. Jain, H. Miyaoka, S. Kumar, T. Ichikawa, Y. Kojima, Int. J. Hydrogen Energy 42 (2017) 24897–24903.
[210] F.B. Juangsa, M. Aziz, Int. J. Hydrogen Energy 44 (2019) 17525–17534.
[211] C.D. Zeinalipour-Yazdi, J.S.J. Hargreaves, S. Laassiri, C.R.A. Catlow, Phys. Chem. Chem. Phys. 20 (2018) 21803–21808.
[212] J.G. Chen, R.M. Crooks, L.C. Seefeldt, K.L. Bren, R.M. Bullock, M.Y. Darensbourg, P.L. Holland, B. Hoffman, M.J. Janik, A.K. Jones, M.G. Kanatzidis, P. King, K.M. Lancaster, S.V. Lymar, P. Pfromm, W.F. Schneider, R.R. Schrock, Science (Washington, DC, United States) 360 (2018) 873.
[213] S. Giddey, S.P.S. Badwal, A. Kulkarni, Int. J. Hydrogen Energy 38 (2013) 14576–14594.
[214] L. Wang, M. Xia, H. Wang, K. Huang, C. Qian, C.T. Maravelias, G.A. Ozin, Joule 2 (2018) 1055–1074.
[215] G. Marnellos, S. Zisekas, M. Stoukides, J. Catal. 193 (2000) 80–87.
[216] K. Imamura, M. Matsuyama, J. Kubota, ChemistrySelect 2 (2017) 11100–11103.
[217] K. Aika, M. Kumasaka, T. Oma, O. Kato, H. Matsuda, N. Watanabe, K. Yamazaki, A. Ozaki, T. Onishi, Appl. Catal. 28 (1986) 57–68.
[218] K. Imamura, J. Kubota, Sustain. Energy Fuels 2 (2018) 1278–1286.
[219] K. Imamura, J. Kubota, Sustain. Energy Fuels 3 (2019) 1406–1417.
[220] J.M. McEnaney, A.R. Singh, J.A. Schwalbe, J. Kibsgaard, J.C. Lin, M. Cargnello, T.F. Jaramillo, J.K. Noerskov, Energy Environ. Sci. 10 (2017) 1621–1630.
[221] X. Chen, N. Li, Z. Kong, W.-J. Ong, X. Zhao, Mater. Horiz. 5 (2018) 9–27.
[222] G.N. Schrauzer, T.D. Guth, J. Am. Chem. Soc. 99 (1977) 7189–7193.
[223] Y. Hao, X. Dong, S. Zhai, H. Ma, X. Wang, X. Zhang, Chem. Eur. J. 22 (2016) 18722–18728.
[224] Y. Zhao, Y. Zhao, R. Shi, B. Wang, G.I.N. Waterhouse, L.-Z. Wu, C.-H. Tung, T. Zhang, Adv. Mater. (Weinheim, Germany) 31 (2019) n/a.
[225] L.F. Greenlee, J.N. Renner, S.L. Foster, ACS Catal. 8 (2018) 7820–7827.
[226] S.Z. Andersen, V. Colic, S. Yang, J.A. Schwalbe, A.C. Nielander, J.M. McEnaney, K. Enemark-Rasmussen, J.G. Baker, A.R. Singh, B.A. Rohr, M.J. Statt, S.J. Blair, S. Mezzavilla, J. Kibsgaard, P.C.K. Vesborg, M. Cargnello, S.F. Bent, T.F. Jaramillo, I.E.L. Stephens, J.K. Noerskov, I. Chorkendorff, Nature (London, U. K.) 570 (2019) 504–508.
[227] M.R. Shaner, H.A. Atwater, N.S. Lewis, E.W. McFarland, Energy Environ. Sci. 9 (2016) 2354–2371.